Master's thesis

NTNU
Norwegian University of Science and Technology
Faculty of Engineering
Department of Energy and Process Engineering

Vilde Eikeskog

Analyses and Evaluation of the Heat Pump Based Energy Supply System Integrating Short- and Long Term Storages

Analyses of Sizing and Operation

Master's thesis in Energy and Environmental Engineering
Supervisor: Natasa Nord
June 2020

NTNU
Norwegian University of Science and Technology

Preface

This master thesis is written during the spring semester 2020 at the Department of Energy and Process Engineering at the *Norwegian University of Science and Technology* in Trondheim. The thesis is the final work of a five year master degree in "Energy and Environmental engineering" and amounts 30 credits.

I would like to thank my supervisor, professor Natasa Nord for guidance and reflections during the semester. Nord have provided good advice for all of my questions and her feedback have been very valuable. When my motivation have been low due to the COVID-19 situation she have also been a great inspiration for continuing the work. I would also like to thank Mohammad Shakerin for great advice and explanations throughout the semester. Both Nord and Shakerin have been supportive and shown great interest in my work, for that I am forever grateful.

The process of writing this assignment have been meaningful and I have learned a lot about modelling and heating systems. The most time consuming part have been to create the mathematical model of the thermal energy system. The semester have been unlike any other due to the COVID-19 situation and most of the assignment is written from my room in Trondheim.

Abstract

Thermal energy systems that provide heating and cooling to a building or area have become more complex over the last decade. The cooling demand for buildings in Norway has increased, and this has resulted in more complex thermal energy systems that require both heating and cooling simultaneously. Heat pump technologies can provide heating and cooling at the same time, and therefore it is often a beneficial solution for providing thermal energy to a building.

From a review of existing thermal energy models and applied thermal energy plants in Norway, a model of a ground source heat pump in a heating and cooling plant integrating long- and short term energy storage is developed. The model consist of three sub-models; a borehole configuration, a heat pump, and a water storage tank. The borehole configuration works as a seasonal thermal energy storage thermally charged during summer and drained during the winter. The water storage tank is connected between the heat pump and the heating system and work as a short term energy storage to obtain smooth operation of the system by reducing the disturbances. The model is used to perform analyses of several strategies for sizing the components, control strategies, various loads, and different compressors. Two distinct loads of heating and cooling demand are used to evaluate the model for loads with significant seasonal differences and a more constant demand. From the analyses in the model, the ratio of the cooling and heating demand influences the energy balance in the borehole storage. If the ratio is too small the borehole configuration will become supercooled with time. The temperature lift of the compressor is significant to the performance of the heat pump and the performance increase with a reduced temperature lift.

Sammendrag

Termiske energisystemer som leverer oppvarming og kjøling til en bygning eller et område har blitt mer kompliserte det siste tiåret. Kjølebehovet for bygninger i Norge har økt, og dette har resultert i mer komplekse termiske energisystemer som krever både oppvarming og kjøling samtidig. Varmepumpeteknologier kan levere oppvarming og kjøling på samme tid, og derfor kan det være gunstig løsning for å levere det termiske energibehovet som er ønsket.

Fra en gjennomgang av eksisterende modeller av termiske energisystemer og anvendte termiske energisystemer i Norge utvikles en modell av en bergvarmepumpe i et varme- og kjølesystem som integrerer langsiktig og kortvarig energilagring. Modellen består av tre delmodeller; en brønnpark, en varmepumpe og en varmelagringstank. Borehullskonfigurasjonen fungerer som et sesongbasert termisk energilager som termisk lades i sommersesongen og tappes i vintersesongen. Varmelagringstanken er koblet mellom kondenseren og varmesystemet og fungerer som en kortvarig energilagring for å oppnå jevn drift av systemet ved å redusere forstyrrelsene. Modellen brukes til å utføre analyser av flere strategier for dimensjonering av komponenter, kontrollstrategier, forskjellige belastninger og forskjellige kompressorer. To ulike belastninger med oppvarming og kjøling brukes til å evaluere modellen for en belastning med store sesongmessige forskjeller og en belastning med mer konstant etterspørsel gjennom året. Fra analysene i modellen kan det konkluderes at forholdet mellom kjøle- og varmebehov påvirker energibalansen i brønnparken. Kompressorens temperaturløft er avgjørende for ytelsen til varmepumpen.

Contents

Figures

Tables

Introduction

The building and construction sector is responsible for 40 % of the direct and indirect CO_2 emissions in the world and the sector is responsible for one-third of the global energy consumption (IEA 2020). This means that the building and construction sector has a high potential for reducing energy consumption and emissions. The use of fossil fuels must be reduced, and renewals must increase to reduce the consumption and the emissions

Several thermal energy systems for one or several buildings are based on heat pump technologies. Norway has a cold climate, and supplying buildings with sufficient heat has been the main priority throughout time. New buildings are more insulated and airtight, and they accommodate more massive computer servers and heat-generating equipment, this has resulted in increased cooling demand. Heat pumps can cover both heating and cooling demand simultaneously and can, for this reason, benefit as a right solution for thermal energy supply systems. As the thermal energy supply systems are getting more advanced control, and the heating and cooling demand for the building is more detailed, the complexity of a thermal energy system increase. Measurements and practical results from thermal energy systems with a heat pump have shown issues regarding the implementation of such solutions. Existing work on this topic shows that several models have been established to perform research on thermal energy systems. The method and the degree of complexity of the models depend on the research questions that are raised. Some models are made in advanced simulation programs, while others are constructed from manufacturer data or actual measurements.

The master's thesis aims to establish a model of a heat pump based energy supply system integrating short- and long term storage and using the model to perform analysis and evaluations of the system. Several research questions have been investigated in the model to improve the model and evaluate the overall thermal energy system. By changing the heating and cooling loads and their ratio, it would be possible to estimate the long term storage sizing and

operation. It is assumed that the reader of this master's thesis has knowledge regarding thermal energy systems and thermal energy storage.

1.1 Thesis Outline

This master's thesis will evaluate an overall thermal energy system similar to applied systems in Norway with several operational conditions depending on the demand. The thermal energy system will use a ground source heat pump with vertical boreholes. The thermal energy system is evaluated by using a MATLAB model. The mathematical model is built by creating three sub-models of the three main components in the system; one sub-model for the boreholes, that work as a long term thermal energy storage, the second sub-model is the heat pump, and the third sub-model is the water storage tank, that works like a short term energy storage. To begin with, a theoretical background is presented, consisting of a brief review of existing literature on the topic and examples of models that are made before. Then, the mathematical model's documentation is presented, followed by the research questions that were analyzed in the model. To obtain useful data for the heat pump capacities and the heat pump performance, a software delivered from the refrigeration and air conditioning technology manufacturer BITZER is used. The model has limited input, and therefore assumptions and calculations must be made to achieve a good model of the system.

1.2 Method

The thesis is based on science within Energy and Process engineering. Fundamental physics and thermodynamic principles were used to develop a model of a thermal energy system. Each component of the system is modeled separately, and then the components are connected. The components are modeled using a dynamic-state approach as well as steady-state and regression models. Relevant performance data for the compressors have been collected from the BITZER software, and input data for the outdoor temperature and thermal energy demand is obtained from previous measurements. Modeling of a thermal energy system is complex, and a set of assumptions have been made to obtain

the mathematical model.

1.3 Structure and Contents

The master thesis is divided into 9 chapters:

Chapter 1 - Introduction
Describe the motivation, goal, method and structure of the assignment.

Chapter 2 - Theoretical Background
Presents heat pump systems and existing research on modeling thermal energy systems.

Chapter 3 - Applied Thermal Energy Systems in Norway
Introduce existing thermal energy systems in Norway.

Chapter 4 - Method for Modeling the Thermal Energy System
Description and documentation of the model that is built.

Chapter 5 - Results of Base Case Model with Two Heating and Cooling Loads
Presents the base case results with two loads and remark some issues of the model.

Chapter 6 - Research Questions in Model
Presents several research questions for further analyses.

Chapter 7 - Results of Research Questions
Presents the results for several research questions for further analyses

Chapter 8 - Discussion
Discussion of results

Chapter 9 - Conclusion
Conclusion and further work

Theoretical background

This section consists of theoretical background for the main components in a ground-source heat pump system with integrated thermal energy storage. A short review of methods for modeling and existing models of thermal energy plants are presented.

2.1 Heat Pump

A heat pump converts heat from a low-temperature heat source to a higher temperature heat by adding power. The heat pump process is based on the principle that fluid temperature will increase with compression and decrease with expansion. A heat pump consists of an evaporator, a compressor, a condenser, and an expansion valve. The components are connected in a closed circuit with a refrigerant with desired thermodynamic properties. There is a heat source connected to the evaporator that delivers low-temperature heat to the system. Typical heat sources are outdoor air, seawater, and geothermal energy. The refrigerant at a low temperature is compressed in the compressor, and the temperature increases. The condenser will transfer heat to the heating system. The high-temperature heat from the condenser covers most of the heating demand, while the low-temperature energy on the evaporator side covers the cooling demand. The purpose of the evaporator is to absorb heat from the heat source by evaporation of the refrigerant. At the inlet of the evaporator, the refrigerant is liquid and have low pressure and temperature. When the heat from the heat source is transferred, the refrigerant evaporates and absorbs the heat. At the evaporator's outlet, the refrigerant has evaporated into superheated steam with low pressure and temperature. The compressor maintains a continuous suction of superheated steam from the evaporator to obtain heat transfer from the heat source to the refrigerant in the evaporator. When the refrigerant enters the compressor in the heat pump cycle, it is compressed to a higher pressure and temperature. At the compressor outlet, the steam is overheated. Compressors have an operating range that the compressing process

must be performed within. An example of such an operating range is shown in figure 2.1. The operating range is given by the evaporating and condensing temperature. The grey line expanding the operating area shows the operating range if the extra cooling capacity is implemented.

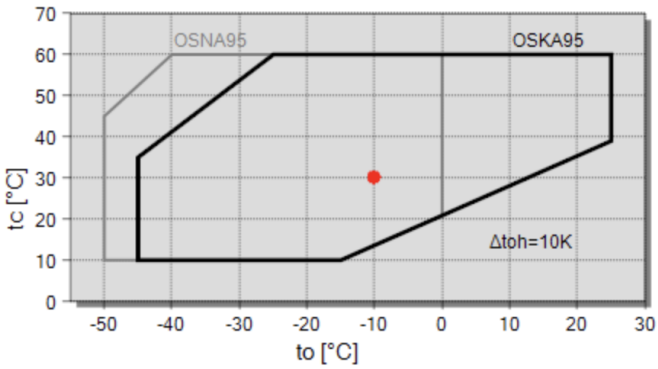

Figure 2.1: Example of operating range for a compressor obtained from the Bitzer software

The coupling of the compressor and motor can be done in three ways; hermetic, semi-hermetic, or open. In a hermetic compressor, the compressor and motor are coupled in the same case, which is closed and can not be opened. In a semi-hermetic compressor, the compressor and motor are coupled in the same case, but the case can be opened for service. Open compressors have separate units for the compressor and the motor. There are different types of compressors; reciprocating, screw, scroll, and turbo compressors. The condenser's purpose is to transfer heat from the refrigerant to the secondary side that will supply the heating system. The heat transfer happens by cooling the superheated steam with high pressure and high temperature to the dewpoint, and when the refrigerant condenses heat is released.

2.1.1 Sizing a Heat Pump

The heating and cooling demand of a building are dependent on the weather conditions. Therefore it is common to implement weather data as an input when

the heating and cooling demand is calculated. Weather data is local data of the weather in an area. It can be obtained from typical values from the past, it can be continuous recordings of the present, or it can be projections of the weather to come. Weather data can, for instance, include temperature, wind, day- and sunlight data. They can include or exclude extreme conditions. The resolution of weather data can vary from monthly data to sub-hourly data(Carlucci 2019).

To size a thermal energy system, the heating and cooling demand of a building or area must be developed. The heating demand consists of both space heating and domestic hot water. The net heating demand for space heating is calculated by adding transmission losses, infiltration losses, and losses from ventilation and then subtract the internal heat loads, heat from users, and radiation from the sun. The space heating demand has seasonal differences, while the domestic hot water demand is close to constant throughout the year (Stene 2019a). The cooling demand occurs when the indoor temperature becomes too high. The cooling demand can be divided into two categories; climate cooling and process cooling. Climate cooling is the seasonal cooling demand due to warm weather and solar radiation. Process cooling is a constant demand due to heat from, for example, server rooms or other processes that continuously generate heat.

The size of a heat pump is determined by the heating and cooling demand. The heating and cooling demand are calculated from weather data, the standard of the building envelope, and the building's internal loads. When the heating and cooling demand is calculated the size of the heat pump can be determined. The highest demand will be the decisive factor in dimensioning the heat pump. A duration curve of the demand for a building is obtained to present the heating and cooling demand. The heat pump will cover the baseload, which consists of most of the energy demand, while the peak load unit will cover the peaks and serve as a back-up. Heat pumps have a high specific investment cost, and a low specific operation cost and the peak load have low specific investment cost but high specific operation cost. The optimal coverage combination is the combination of baseload and peak load that results in the lowest annual cost. When sizing a heat pump, two coverage ratios should be taken into account, the power coverage β and the energy coverage α. The heat pump should cover β = 40-70 % of the maximum power and α = 70-95 % of the energy. The remaining demand should be covered by the peak load. The peak load often

serve as a backup in the system, and must cover the power demand $\beta_{\text{peak}} = 100$ %. The cooling demand has increased over the years as the buildings are more insulated, and more heat-generating equipment is implemented. The heating demand is still the dominating load for most of the thermal energy systems (Stene 2019a).

2.2 Water Storage Tank

A water storage tank, also called a water storage tank, is a tank connected between to units in a process to improve the operation by reducing disturbances and obtain better control. (Faanes et al. 2003) separate the water storage into two categories based on the purpose of the tank. The first category is a tank that intends to reduce or dampen the disturbances from one unit to another. The other category of the water storage tank intends to provide independent operation for parts of the system. A water storage tank in a thermal energy system is usually situated between the condenser and the heat supply system. The heat from the secondary side of the condenser is transported to the water storage tank. In the water storage tank water at a high temperature can be stored before it is distributed to the heating system. A water storage tank acts as a hydraulic separator between the condenser circuit and the heating system. It helps obtain a constant mass flow rate in the condenser circuit and a variable flow for the demand regulated heating system. Independent operation in a heating system can be obtained by shutting down the heat pump and use the thermal energy in the water storage tank to supply the heating system. The purpose of the water storage tank is to reduce the disturbances between the units, reduce power demand, and reduce the compressor's frequent on/off regulation. There are several solutions considering the layout of a water storage tank regarding the connected pipes, heat transfer, and heat generation. One example presented here. The water storage tank can have three connected pipes. The outflow to the heating system is demand dependent and will distribute heat to the heating system. The second outflow will be equal to the constant inflow minus the demand dependent outflow. There is no heat generation inside the tank, so the change in energy will be the sum of the flows and the losses due to convection. Figure 2.2 shows how the water storage tank is connected and an example of the mass balance in the water storage tank. There are numerous layouts for wa-

ter storage tanks and the most common layout include four pipes; one inflow and one outflow on the top to supply the heating system, and one inflow and outflow at the bottom to ensure mass balance.

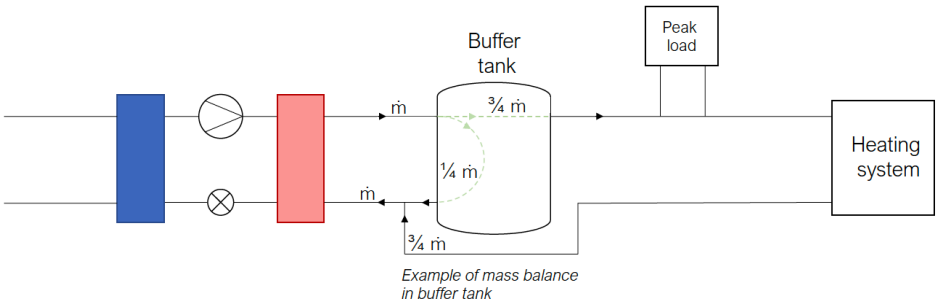

Figure 2.2: water storage tank with one inlet and two outlets (Stene 2020)

There are various solutions for sizing a water storage tank. One solution is to size the tank dependent on the minimum operation step of the heat pump. Another solution is to size the water storage tank from the time the water is stored in the tank, also called the residence time. If the water storage tank is sized by the minimum operation step method, it is sized to have 20-40 $\mathrm{l kW^{-1}}$ at the lowest performance of the heat pump(Stene 2020). If a heat pump has a maximum performance of 100 kW and can perform on 20 % of the capacity, the water storage tank would be sized to be 400-800 l, as shown in equation 2.1.

$$V_{storage,tank} = p_{\mathrm{Qk,min}} \cdot Q_k \cdot V_{specific} \tag{2.1}$$

where

$p_{\mathrm{Qk,min}}$ = Minimum Operation Step [%]
Q_k = Condenser Capacity of Heat Pump [kW]
$V_{specific}$ = Specific Volume, usually 20-40 [$\mathrm{l kW^{-1}}$]

To size the heat pump by the residence time, equation 2.2 is used.

$$\tau = V/\dot{m} \tag{2.2}$$

τ = residence time [h]
V = volume of the tank [m^3]
$\dot{m}$ = nominal mass flow supplied to the heating system [m^3/h]

There is one inflow to the tank, where warm water from the condenser is supplied to the tank with a mass flow $\dot{m}_c$ and temperature T_c. There are two outflows from the tank. The first outflow is the demand dependent water distributed to the heating system. The water distributed to the heating system have a mass flow $x \cdot \dot{m}$ where $x \in [0, 1]$ and a temperature T_c. The second outflow is as the bottom of the tank, this flow is mixed with the return water from the heating system and delivered to the condenser. There is a temperature in the water storage tank so that the temperature of the outflow is lower than the other outflow. There will be some heat loss through the walls of the tank. The water storage tank manufacturer Mibec inform that their tanks have a U-value of 0.22 (Mibec 2020).

2.3 Boreholes

Geothermal heat is thermal energy stored in the ground below the surface. The thermal energy stored in the ground mainly consists of energy from the sun. The ground has a relatively high and stable temperature fifteen meters below the surface, and therefore geothermal heat is considered an excellent heat source for heat pump systems (Ramstad 2017).

The geothermal energy is extracted from the ground by heat exchangers in vertical boreholes. The heat is extracted by the boreholes and delivered to the evaporator side of the heat pump at a relatively high and stable temperature. The boreholes are between 100-350 meters deep, and the heat exchanger is a closed single or double U-pipe, usually filled with an ethanol-based brine. There are also some open borehole systems, but these are not common in Norway (NGU 2020b). The borehole configuration can extract only heat, or it can work as seasonal storage for thermal energy, this depends on the distance between the

boreholes. A borehole configuration for thermal energy can be used to extract heat and store heat when there is surplus heat in the heating system. During summer, when the cooling demand is dominating, excess heat can be delivered back to the boreholes for seasonal thermal energy storage. The heat delivered to the boreholes will result in seasonal temperature changes in the borehole system.

2.3.1 Sizing Borehole Configuration

Sizing a thermal energy borehole storage requires knowledge of the ground properties at the site where the boreholes will be implanted. To size a borehole configuration, a thermal response test (TRT) and an Energy Earth Designer (EED) evaluation should be carried out to ensure energy balance in the relationship of the heat pump and ground properties (Ramstad 2017). The thermal properties of the ground cannot be obtained by measurements on the surface of the ground. The thermal properties of the ground must be obtained by performing a thermal response test. A thermal response test is carried out by drilling a test borehole at the planned depth. From the borehole, the main properties for sizing the borehole storage is obtained. The main properties are the thermal conductivity, the resistance of the ground, and the temperature of the unaffected ground (Reuss 2015). The ground properties are then evaluated in Energy Earth Designer, a program used to evaluate the energy balance and temperature of the borehole storage. This evaluation must be performed in order to avoid too low temperatures and a supercooled borehole storage. If the energy balance in the borehole storage is not obtained from the surplus energy delivered to the storage, other solutions must be implemented. The boreholes can, for example, be charged using heat recovery from greywater, heat from solar collectors, or heat recovery from excess ventilation air.

2.4 Modelling and Application of Ground Source Heat Pumps

There is a considerable amount of research on thermal energy systems with ground source heat pumps. This section presents a review of modeling approaches used to construct a model of ground source heat pumps and thermal

energy systems. There are several ways to model a ground-source heat pump system. Underwood (2016) presents established approaches for modeling ground-source heat pump systems.

Steady-State Models are models where all the parameters are in balance, and there are no internal changes in the system. A Steady-State model can be developed to calculate the heat pump compression cycle. Input data is used to calculate the desired parameters using thermodynamic equations and tables. If input data is unknown, a guess can be made, and an iterative calculation can be performed to find a good estimate for the guessed parameter.

Dynamic-State Models are constructed to observe variations in a system over time. Dynamic-State modeling can be carried out from transfer functions and distributed parameter modeling. Discretization can be used in systems were the control volume is dependent on changes in one axial direction.

Regression Models can be constructed by performing regression on equations or curves obtained by data for the equipment. There are two sources of required data; experimental data and data from the manufacturer. Manufacture data are often generated from simulated models. The data is idealized and is not affected by the influence of the layout and installation of the actual system. Experimental data can be more realistic as the data is obtained from measurements in an actual system. Models that are constructed using a regression approach can have high accuracy, but they are also limited to the parameters used to perform the regression.

Several software programs can be used for modeling ground-source heat pumps and thermal energy systems. Persson et al. (2016) presents software programs for modeling and simulation of ground source heating and cooling systems. The software that can be used is Energy Earth Designer, TRNSYS, Polysun, IDA ICE, MATLAB with the Simulink package Carnot and Modelica. Most of these systems are best implemented to investigate the influence of the borehole storage in the thermal energy system. They are not detailed enough for investigating the boreholes themselves.

2.4.1 Models of Thermal Energy Systems

Alimohammadisagvand et al. (2018) uses the building simulation tool IDA ICE to model a ground-source heat pump with two water storage tanks, one for domestic hot water and one for space heating for a multi-zoned residential building. The tanks are modelled as one dimensional stratification tanks with 10 layers. The model is used to investigate rule-based control algorithms to reduce energy consumption without reducing the thermal comfort of the occupants.

Madani et al. (2011) build a model of a thermal energy system with an integrated ground source heat pump and a water storage tank. The model is developed by combining several sub-models for the components in the system in either TRNSYS or EES and connects the sub-models after.

Kim et al. (2013) presents a model of a ground source heat pump built on manufacturer data. The method starts with the entering water temperature and the leaving water temperature and compare the actual performance of the heat pump with the idealized data.

Claesson et al. (2011) presents an analytical method of calculating the fluid temperature in boreholes. The method can be implemented to a mesh grid of boreholes to calculate the boreholes influence on each other. Cadau et al. (2019) presents a model on a multi-node dynamic model of a stratified water storage tank. The model is implemented in MATLAB/Simulink and the results conclude that the model of the stratified tank can be transmitted to the results of an actual tank.

2.4.2 Dynamic Modelling of Thermal Energy Systems

A system can be described by a mathematical model. The mathematical model is a set of equations that describe a systems behavior over time. To develop a mathematical model require well defined boundaries of the system and assumptions must be made to simplify the model. When the boundaries and assumptions are made a balance law must be obtained to implement the physical processes in the system (Haugen 2003). The general balance law that calculate the change of a parameter can be expressed by adding the inflows, extract the outflows and add generated material in the system. This is expressed in equation 2.3.

$$\frac{d(material)}{dt} = \sum inflows - \sum outflows + \sum generated \tag{2.3}$$

When modeling thermal systems the balance law is an energy balance that can be expressed as in equation 2.4.

$$\frac{dE(t)}{dt} = \sum_i \dot{Q}_i(t) \tag{2.4}$$

E = Thermal energy [J]
$\dot{Q}_i$ = Heat flow [J/s]
t = Time [s]

where The energy is assumed to be proportional with temperature and mass flow. This means that the energy can be expressed in multiple ways as presented in equation 2.5.

$$E = c_p \dot{m} T = c \rho V T = C T \tag{2.5}$$

where

c_p = Specific heat capacity [$\mathrm{J\,kg^{-1}\,K^{-1}}$]
m = Mass [kg]
V = Volume [$\mathrm{m^3}$]
ρ = Density [$\mathrm{kg/m^3}$]
C = Total heat capacity [$\mathrm{J\,K^{-1}}$]

Applied Thermal Energy Systems in Norway

In Norway there are several ground-source heat pump systems. This section will present five existing ground source heating systems and how they work. The systems are presented from oldest to newest. After the presentation of these systems follows a summary of the main the challenges in these systems.

3.1 Vulkan energy plant

Vulkan energy plant is a large thermal energy plant at the Vulkan area in Oslo. The plant consist of five heat pumps, an ice storage, solar collectors and district heating to cover peak loads. The plant cover the cooling of food, heating demand, preheating of domestic hot water, snow melting of pedestrian zones and the cooling demand for a food court, office buildings, hotels and apartments with a total area of 38 500 m^2. The thermal energy plant at Vulkan is very complex and operation require high competence in facility management.

There are two borehole storage for the thermal energy plant and they amount 62 boreholes at 300 m each. Heat pump 1 and 2 are provided with heat from the boreholes and in over all heating mode heat pump 1 and 2 deliver heat for space heating, preheating of domestic hot water and snow melting. In overall cooling mode the surplus heat on the condenser side of heat pump 1 and 2 are sent to the boreholes for thermal charging of the borehole storages. Heat pump 4 and 5 are connected in parallel and work as a cooling plant for the food in the food court. The waste heat from the cooling plant is sent back to the evaporator side of heat pump 4 and 5. Heat pump 3 is connected in cascade with heat pump 4 and 5, this means that the condenser heat from heat pump 4 and 5 at around 25 °C is delivered to the evaporator side of heat pump 3. The heat generated in heat pump 3 cover the heating demand with heat pump 1 and 2. In overall cooling mode the ice storage is used to cover the peak demand for cooling. The

solar collectors deliver heat to the heating system in overall heating mode and send heat back to the boreholes for thermal charging during overall cooling mode. A simplified system scheme of the Vulkan energy plant is attached in appendix A figure A.2.

The thermal plant have both seasonal heating and cooling demands; space cooling, space heating, snow melting, and heating and cooling demands that are more or less constant over the year; domestic hot water and cooling of food. Based on the measurements of the thermal energy use in 2017, Daniel Rohde simulated the heat extracted and delivered to the borehole storages over the year. The results can be seen in figure 3.1. The extracted heat is a bit larger than the heat delivered to the boreholes, which can influence the borehole storage with time. It can be seen that the heat delivered from the solar collectors is low (Rohde 2019).

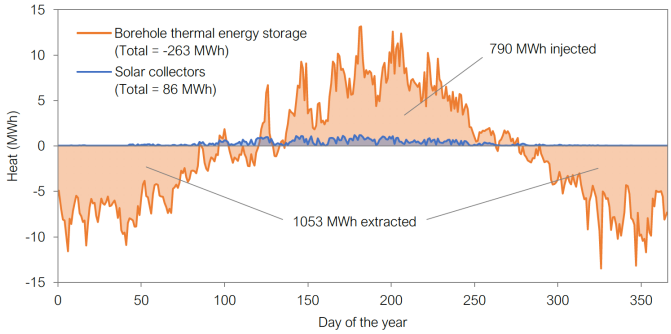

Figure 3.1: The simulated energy balance in the borehole storage based upon measured data (Rohde 2019).

3.2 The SWECO Building

The SWECO building is an office building in Bergen housing a food store on the first floor. The building has a total area of 18 000 m^2 and was finished in 2016. The waste heat from the cooling plant in the food store is used in the system to preheat domestic hot water. The borehole storage deliver heat to the evaporator side of the heat pump. The cooling system is connected in parallel with the evaporator circuit so the return flow from the cooling system is mixed with the

flow from the boreholes before the evaporator. The heat pump is dimensioned from the maximum cooling demand as is was expected that the cooling demand would be very high. The heat pump use ammonia as refrigerant and the heat from the heat pump cover the space heating of the building and preheating of the domestic hot water together with the waste heat from the cooling plant in the food store. District heating is used to lift the hot water temperature. A simplified scheme of the system can be found in appendix A figure A.3.

An issue with the thermal energy system of the SWECO building is the large reduction of -70% from the pre-calculated cooling demand to the actual cooling demand (Aaberg 2019).

3.3 Moholt 50 | 50

Moholt 50 | 50 is an extension of the student residence area at Moholt in Trondheim. The extension was finished in 2016 and consist of five nine story apartment buildings, a kindergarden, a common laundry, a library and a fitness center with a total area of 23 400 m^2. The thermal energy plant consist of a borehole storage, three heat pumps and solar collectors and a grey water heat exchanger. The plant cover the heating demand for ventilation air, domestic hot water and snow melting of pedestrian zones. Free cooling from the boreholes are used to cover the cooling demand of ventilation air (Meisler 2020). The 23 boreholes at 250 m deliver heat to the evaporator side of the heat pumps. The surplus heat from the heat pumps after covering the demand is used to pre-heat domestic hot water for older student apartments. The borehole storage is charged with heat from a grey water heat exchanger, solar collectors and from heat recovery of the ventilation air. A simplified scheme of the system can be found in appendix A figure A.4.

3.4 KIWI Dalgård

KIWI Dalgård is a food store in Trondheim with high ambitions regarding sustainable solutions. The thermal energy system consist of a CO_2 cooling plant for the cooling and freezing of products in the store and a ground source heat pump with eight boreholes at 264 m to cover heating demand. The purpose of

the system is that the waste heat from the gas cooler can cover a high fraction of the heating demand in the store and the ground source heat pump can cover the remaining demand in the store and then deliver most of the heat to the nearest residence buildings. In overall cooling mode the CO_2 cooling plant send waste heat back to the boreholes for thermal charging. A simplified scheme of the thermal energy system is shown in appendix A figure A.5. The waste heat from the CO_2 cooling plant cover 92% of the heating demand in the store and the borehole storage is in thermal balance. The residential buildings that receive the surplus heat have a higher temperature level in the heating system than the heat pump can deliver, and the utilization of the surplus heat is not well conducted (Aaberg 2018).

3.5 Otto Nielsens Vei 12 E

Otto Nielsens Vei 12E is an office building in Trondheim that was finished in 2017. It is an extension of an existing office building. The tenant of the building have a high demand for process cooling and the waste heat from the cooling generation is delivered to the connected neighbor building for space heating. The thermal energy system consist of a borehole storage with 25 boreholes at 258 m that deliver heat to the evaporator side of the heat pump. The heat pump cover the space heating, preheating of domestic hot water, snow melting, process cooling and space cooling. Waste heat is delivered to the neighbor office building and to the boreholes for thermal charging. If the borehole temperature is above 20 °C, the surplus heat is released through the snow melting system. A simplified scheme of the thermal energy system is presented in appendix A figure A.6. The main issue with the thermal energy system is the temperature level of the surplus heat delivered to the neighbor building. The temperature is very high, and the heat transfer is not as efficient as it could be. The high temperature level reduce the seasonal performance factor. (Alfstad 2018).

3.6 Challenges in The Applied Thermal Energy Systems

Variation in pre-calculated and actual heating and cooling demand is a challenge as the pre-calculated demand is used to size the system. If there are high deviations the system can be sized incorrectly.

Temperature level of the system is influencing the heat pump performance and if the temperature level is too high this can tear on the compressor and is will reduce the overall performance of the system.

Supercooling of borehole storage can become an issue if the ratio between the cooling and heating demand is too low. The temperature of the borehole storage should be monitored to ensure that the temperatures are not too low.

Method for Modeling the Thermal Energy System

Chapter 4 presents the mathematical model that was developed. The model was divided into three main parts that is presented separately. The first sub-model is the borehole configuration, which operate as a seasonal thermal energy storage and is presented as the third sub model. The second sub-model is the heat pump and how the evaporator, condenser and compressor capacities are obtained. The third sub-model is the water storage tank that operate as a short-term thermal energy storage. The sub-models are based upon hourly weather data and heating and cooling demand incorporated with thermodynamic principles. This chapter explains the model, and significant equations and schemes. Information flow charts are utilized to obtain a sufficient detail level. The model presented in this chapter is the basecase model. The results developed from the model are presented in the following chapters.

4.1 System Layout and Introductory Part

This section begins with explaining the layout of the thermal energy system that is used for building the model. Then

4.1.1 Plant Configuration and Operational Conditions

The model that was built in this master's thesis was based on a typical ground-source heat pump plant integrating long- and short term energy storage. The heat pump configuration have different operational conditions depending on the seasonal differences in the demand. Figure 4.1 presents the layout of the thermal energy system that was modelled.

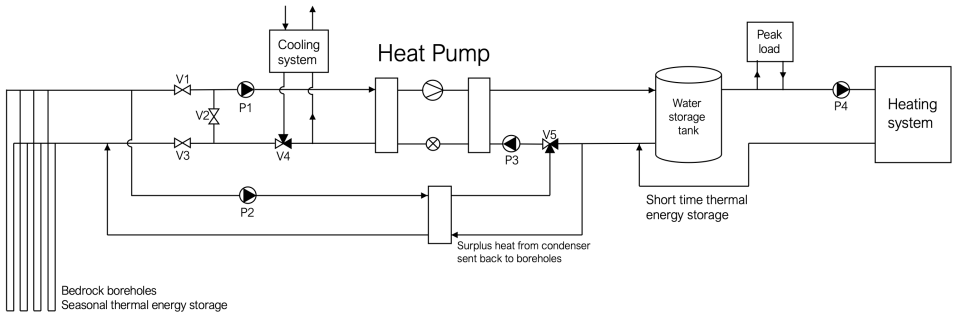

Figure 4.1: General heat pump configuration with bedrock boreholes

The heating system is where the heat generated by the thermal energy system is supplied to cover the demand. While the heating system usually consists space heating from of radiators and heating of ventilation air and heating of domestic hot water, these loads are assembled into one large heating demand. The same applies to the cooling demand which usually consist of both process cooling and cooling ventilation air. The thermal energy system have three operational conditions; overall heating mode, overall cooling mode and free-cooling mode.

Overall Heating Mode

The system operate in overall heating mode when the heating demand is larger than the cooling demand. Figure 4.2 shows the operational conditions. The evaporator is supplied with heat from the boreholes and the heat pump generate heat that is distributed to the heating system on the condenser side. If the heat pump is not able to cover the heating demand, the peak load will be used to cover the remaining demand. After the evaporator, the brine will deliver heat to the cooling system. The cooling demand in overall heating mode is usually process cooling of for example a data center.

Overall Cooling Mode

The system operate in overall cooling mode when the cooling demand is larger than the heating demand. Figure 4.3 presents a scheme of the operational conditions in overall cooling mode. The heat pump supplies the cooling system

with low temperature brine on the evaporator side. The heating demand will be covered by the condenser heat. The surplus heat from the condenser will be sent back to the boreholes for seasonal thermal energy storage. In overall cooling mode the borehole thermal energy storage is charged with heat so that the temperature will increase.

Free-Cooling Mode

The system operate in free-cooling mode when the heating demand is zero and the cooling demand can be covered by the borehole thermal energy storage. In free cooling mode the heat pump can be turned off. Figure 4.4 presents the operational conditions in free-cooling mode.

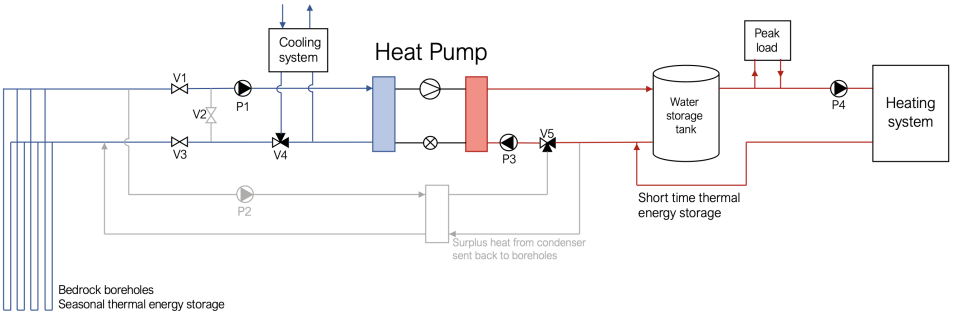

Figure 4.2: Heat pump configuration in overall heating mode

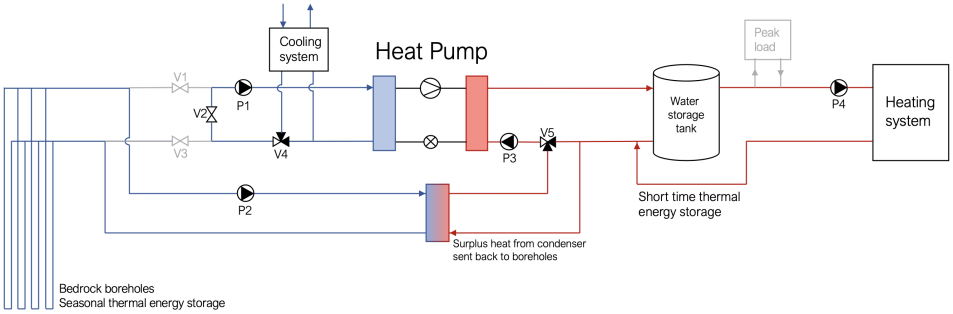

Figure 4.3: General heat pump configuration in overall cooling mode

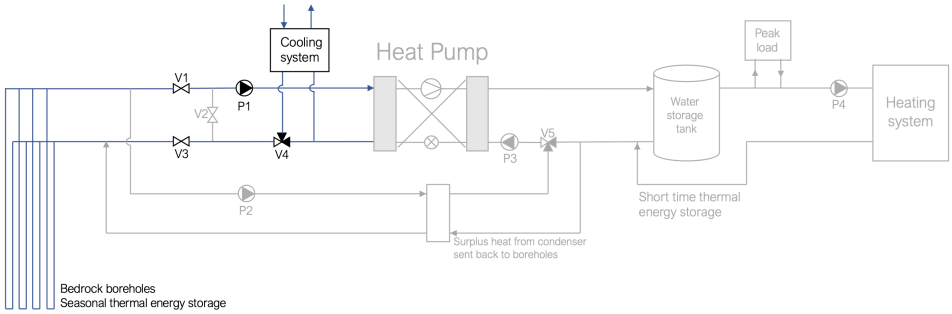

Figure 4.4: General heat pump configuration in free-cooling mode

4.1.2 Introductory Part

Before the first sub-model there is an introductory part where input data is loaded and the primary set-point temperatures for the thermal energy system is set. The input data that is loaded is presented in table 4.1.

Input data	**Name**	**Unit**
Heating demand at hourly interval	Q_{hl}	kW
Cooling demand at hourly interval	Q_{cl}	kW
Outdoor temperature at hourly interval	T_{out}	°C
Condenser coefficients	$Condenser_{Coefficients}$	-
Evaporator coefficients	$Evaporator_{Coefficients}$	-
Compressor coefficients	$Compressor_{Coefficients}$	-
Condenser temperature coefficients	$CondenserTemp_{Coefficients}$	-

Table 4.1: Input data for the model of the thermal energy system

The heating and cooling demand are input data in the model. The loads are calculated or measured in advance. For the heating and cooling demand, the model is tested with two distinct loads, the two loads and their particular characteristics are presented in chapter 5. The time step resolution of the demand is hourly intervals. The outdoor temperature T_{out} was obtained from a weather

data file that have logged the outdoor temperature each hour for a year. Figure 4.10 shows the outdoor temperature that was used as an input in the model.

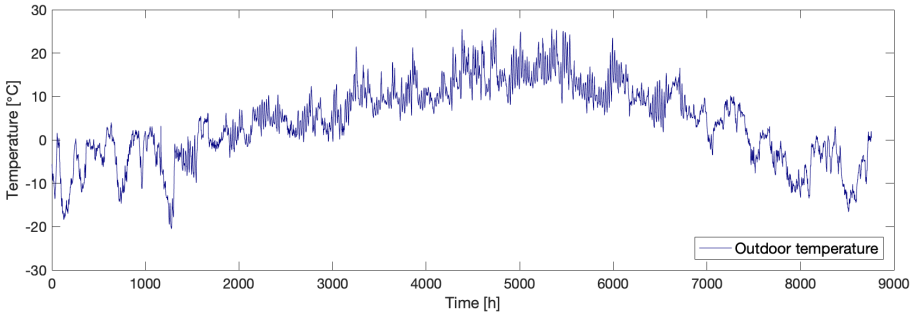

Figure 4.5: Hourly outdoor temperature over a year that is loaded as an input in the model

Evaporator, condenser and compressor coefficients are input data loaded in the introductory part. The coefficients are obtained from the Bitzer software. Bitzer is a manufacturer that deliver refrigeration and air conditioning technologies with competence in developing compressor technology (BITZER 2020). The coefficients are obtained by performing a regression on manufacturer data from several operating conditions.

4.2 Modeling the Boreholes

The heat source of the thermal energy system is thermal heat from the ground. The heat is extracted by heat exchangers in several vertical boreholes connected in parallel. The borehole configuration act as a seasonal thermal energy storage. In this section the modelling of the borehole storage is presented. The borehole configuration was modelled as a control volume using a deterministic and dynamic-state approach. Figure 4.6 shows a simplified scheme of the borehole configuration and its connection to the thermal energy system.

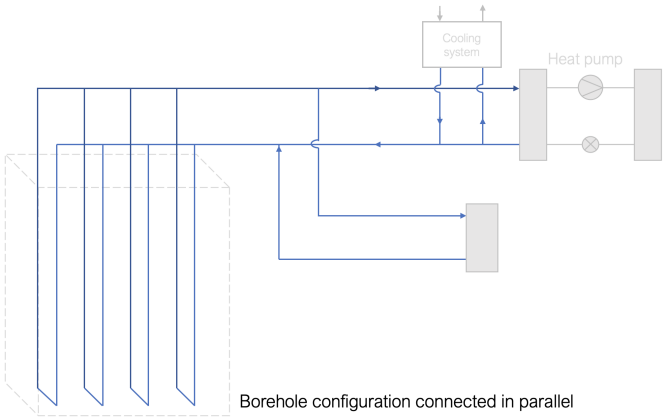

Figure 4.6: Simplified scheme of borehole configuration

4.2.1 Sizing the Volume of the Borehole Configuration

The sizing of a thermal energy borehole storage was presented in chapter 2.3.1. Since the model is not located at a specific area the thermal ground properties can not be obtained from a thermal response test and the properties are instead assumed from typical values in Norway. The sizing of the borehole configuration was performed by utilizing a "rule of thumb" to calculate the total meters of boreholes from the evaporator capacity. In general, this is not sufficient for sizing a borehole storage (Ramstad 2017). An EED simulation was carried out later in the thesis to obtain an impression of how realistic the sizing was. The thermal properties of the ground are presented in table 4.2.

Parameter	**Name**	**Value**	**Unit**
Heat effect	q_{ground}	40	$W\,m^{-1}$
Thermal conductivity	λ_{ground}	2.62	$W\,m^{-1}\,K^{-1}$
Temperature in unaffected ground	T_{ground}	6	°C
Length to unaffected ground	l	10	m

Table 4.2: Thermal properties of the ground

The thermal energy borehole storage was sized from the properties of the ground and the heat pump. Note that this calculation of sizing the boreholes is a mathematical approach and experience was not taken into account. Equation 4.1 and 4.2 are used to calculate the evaporator capacity and then 4.3 calculate the meters of effective boreholes that is required to cover the evaporator capacity.

$$COP = \frac{Q_c}{W} \tag{4.1}$$

$$Q_e = Q_c - W \tag{4.2}$$

$$m_{boreholes} = \frac{Qe}{q_{ground}} \tag{4.3}$$

COP = Coefficient of Performance [-]
Q_c = Condenser Capacity [kW]
W = Compressor Power [kW]
Q_e = Evaporator Capacity [kW]
$m_{boreholes}$ = meter of effective boreholes required [m]
q_{ground} = Specific heat effect in ground [$\mathrm{W\,m^{-1}}$]

Length of the boreholes is usually between 150-300 meters. (Ramstad 2017). The amount of boreholes can then be decided by dividing the total length of effective boreholes with the chosen length for the boreholes. The length and amount of boreholes are calculated. The volume of the borehole storage is essential for further calculations. To obtain a simplified calculation of the total volume, the borehole configuration is modelled as a square configuration of the boreholes with 6 meters distance between each borehole. The distance between each borehole in the square configuration is 6 meters, each borehole have a horizontal surface area of 36 square meters, a graphic example is given in figure 4.7. Note that the components in the figure are not scaled.

When the number of boreholes were calculated a simplified horizontal area was found by multiplying the number of boreholes with the surface area for each borehole. Further, the volume was obtained by multiplying the total horizontal area with the length of the boreholes. The volume was then used to calculate the surface area of the total borehole storage. The calculation is a simplification assuming a square configuration of the boreholes even if the number of boreholes do not add up in a square configuration.

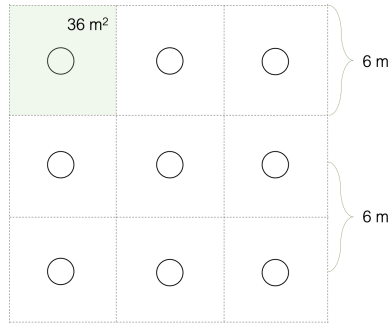

Figure 4.7: Example of borehole configuration with six meters distance between each borehole

4.2.2 Thermal energy calculations for the borehole storage

The borehole configuration is an indirect system with heat exchangers in the boreholes, figure 4.8a shows a simplified scheme of the borehole storage. A control volume approach is used to model the thermal system of the borehole storage. Figure 4.8b present how the control volume is set up. The inflows and outflows for each borehole are combined to inflow and outflow. The direction of the heat transfer to the surrounding ground will depend on the temperature in the borehole storage.

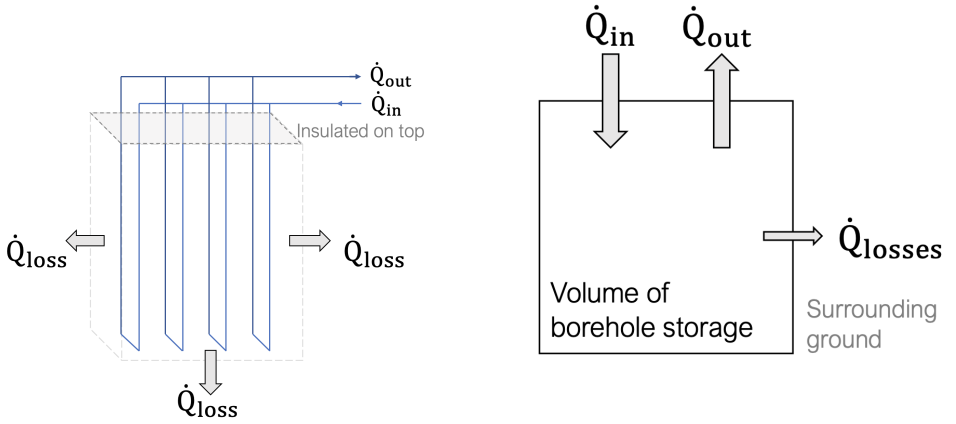

(a) Simplified scheme of borehole configuration, top surface is insulated

(b) Control volume approach for model of thermal energy borehole storage

Figure 4.8: Schemes of the the actual thermal energy flows in a thermal energy borehole storage and the simplified control volume

Equation 4.4 is the heat balance used to model the system. $\dot{Q}_{\text{fromHS}}$ is the heat rate of the brine transported through the boreholes, and $\dot{Q}_{\text{losses}}$ is the heat transfer to the surrounding ground.

$$\frac{dE_{bh}(t)}{dt} = \dot{Q}_{fromHS} + \dot{Q}_{losses} \tag{4.4}$$

It is assumed that the heat transfer from the brine to the borehole storage is ideal and that the temperature of the brine at the outlet of the control volume is equal to the borehole temperature. Equation 4.5 presents the heat rate over inflow and outflow of the borehole configuration.

$$\dot{Q}_{fromHS} = c_p \dot{m} \Delta T = c_p \dot{m} (T_{s,bh} - T_{bh}) \tag{4.5}$$

Fourier's law was used to calculate the heat transfer to surrounding ground. It was assumed that the horizontal area at the top of the borehole storage is insulated. The heat transfer with surrounding ground occur vertically at the bottom of the storage and horizontally at the vertical edges of the storage. Equation 4.6 presents the heat transfer with the surrounding ground.

$$\dot{Q}_{losses} = \dot{q} \cdot A = -\lambda \nabla T \cdot A = -\lambda \frac{dT}{dx} \cdot A = -\frac{\lambda}{dx}\left(T_{bh} - T_{ground}\right) \cdot A \tag{4.6}$$

The change in temperature over time is presented in equation 4.7.

$$\frac{dT_{bh}(t)}{dt} = \frac{1}{c_p \rho V}\left(c_p \dot{m}(T_{s,bh} - T_{bh}) - \frac{\lambda}{dx}\left(T_{bh} - T_{ground}\right) \cdot A\right) \tag{4.7}$$

This was the main equation used in the calculation of the hourly temperature development over a year. To calculate the temperature development a temporal discretization is performed on equation 4.7, where Δt accounts for an hour time step and i represent the current time instance. The temporal discretization is presented in 4.8.

$$\frac{\Delta T_{bh}(i)}{\Delta t} = \frac{1}{c_p \rho V}\Bigg(c_p \dot{m}(i-1)(T_{s,bh}(i-1) - T_{bh}(i-1)) - \frac{\lambda}{dx}\left(T_{bh}(i-1) - T_{ground}\right) \cdot A\Bigg) \tag{4.8}$$

$$T_{bh}(i) = T_{bh}(i-1) + \Delta T_{bh}(i) \tag{4.9}$$

$T_{s,bh}$ is dependent on the operational mode of the heating system. When the system runs in overall heating mode or in free-cooling mode $T_{s,bh}$ is the return temperature after the cooling system, and when the system is in overall cooling mode $T_{s,bh}$ is the temperature of the surplus heat after the heating system on the condenser side. The temperature for $T_{s,bh}$ for the three operational modes are listed in table 4.3.

Operational mode	$T_{s,bh}$
Overall heating mode	$T_{r,CS}$
Overall cooling mode	$T_{r,HS}$
Free-cooling mode	$T_{r,CS}$

Table 4.3: The temperature of the brine at the inlet of the borehole storage

The return temperature for the cooling system $T_{r,CS}$ was calculated from the equation of the cooling demand, the calculation is presented in equation 4.10.

$$T_{r,CS} = T_{s,CS} - \frac{\dot{Q}}{c_p \cdot \dot{m}} \tag{4.10}$$

$\dot{Q}$ = cooling delivered to cooling system [W]
c_p = specific heat capacity [$J\,kg^{-1}\,K^{-1}$]
$T_{s,CS}$ = temperature delivered to cooling system [K]
$\dot{m}$ = mass flow in the cooling system $kg\,s^{-1}$

Figure 4.9 is a flowchart that presents the information flow for the sub-model of the borehole storage. The most important calculations from this section are displayed.

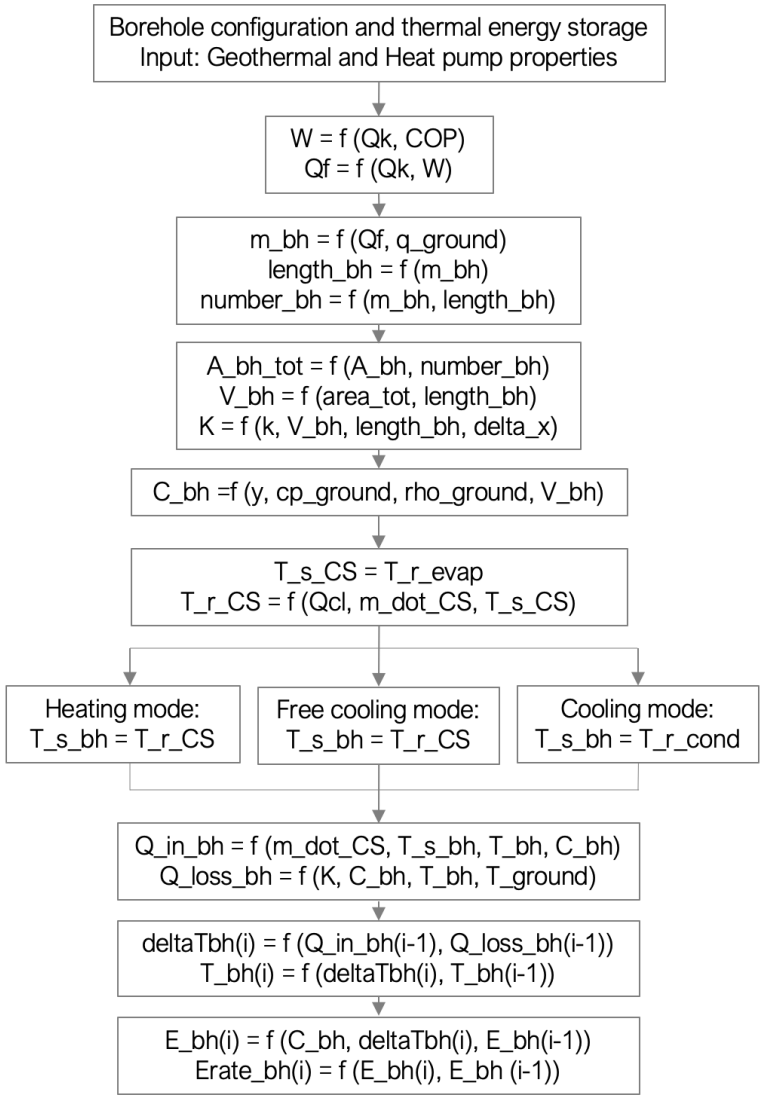

Figure 4.9: Flowchart borehole sub-model

4.3 Sub-Model for the Heat Pump

The second part of the model is the heat pump. Here the evaporator, condenser and compressor capacity was calculated as well as the actual operating power of the components related to the heating and cooling demand. The model consist of a regression model with data from compressor manufacturer BITZER. The coefficients obtained from the regression was uploaded to MATLAB for further steady-state calculations of the operation and performance. Figure 4.10 present a scheme of the heat pump.

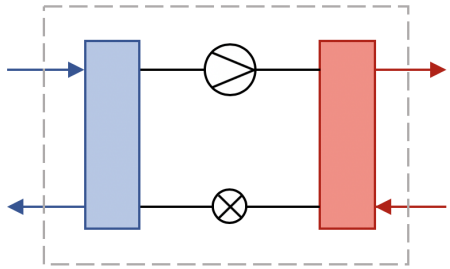

Figure 4.10: Scheme of the heat pump

4.3.1 Set-Point Temperatures in Thermal Energy System

The return temperatures from the evaporator and compressor in the system was set to a constant temperature.

For the heating system in the model it was decided to have two different temperatures dependent on the outdoor temperature. The desired return temperature from the condenser was set to be 55 °C when the outdoor temperature was under 7 °C and 50°C when the outdoor temperature was above 7 °C. The same solution was decided for the cooling system. The return temperature from the evaporator was set to be 7 °C when the outdoor temperature was under 7 °C and 5°C when the outdoor temperature was above 7 °C. A scheme of the system layout with relevant parameters from the MATLAB model can be found in the Appendix A.1.

The temperature difference over the condenser and evaporator was assumed

to be 5 °C. The temperature difference over the condenser and evaporator is used to calculate the refrigerant temperature at the compressor discharge and evaporator. Figure 7.22 shows a scheme of the heat transfer in the condenser and evaporator to and the temperature differences that are assumed. Equation 4.11 and 4.12 shows the calculation.

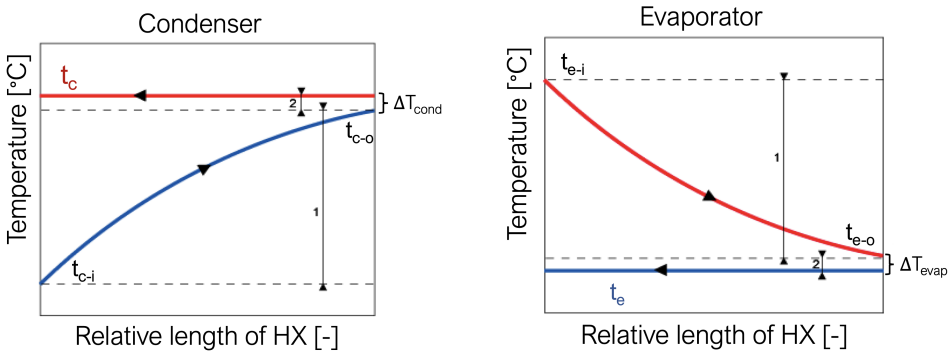

(a) Heat transfer in condenser

(b) Heat transfer in evaporator

Figure 4.11: Heat transfer in condenser and evaporator, where ΔT_{cond} and ΔT_{evap} is marked (Stene 2019b).

$$T_d = T_{s,HS} + \Delta T_{cond} \tag{4.11}$$

$$T_o = T_{s,CS} - \Delta T_{evap} \tag{4.12}$$

4.3.2 Polynomials Derived from the Bitzer Software

In the Bitzer software different compressor types can be selected together with input data regarding the operating conditions. The software calculate cooling and evaporator capacity, COP, mass flow for the relevant compressor. The Bitzer software compute a polynomial for the evaporator, condenser and compressor capacity and the condenser temperature as a function of the temperatures Td and To presented in section 4.3.1, f (Td, To). These polynomials are generated for various operational conditions to generate more data (BITZER Group 2020). From this data, a curve fitting regression is performed to generate functions for

the condenser, compressor, evaporator and condenser temperature capacities. These are functions of the evaporator capacity as a function of To and Td and the condenser capacity, compressor capacity and the condenser temperature as a function of To, Td and the evaporator capacity, f (Td, To, Qcl_0) and the coefficients for these polynomials are loaded into the MATLAB model. Equation 4.13, 4.14, 4.15 and 4.16 show the polynomials used in the model.

$$Q_{cl,0} = q_1 + q_2 T_o + q_3 T_o^2 + q_4 T_o^3 + q_5 T_d^3 + q_6 T_d + q_7 T_d T_o + q_8 T_d T_o^2 \quad (4.13)$$

$$Q_{cd,0} = C_1 + C_2 T_d + C_3 T_o + C_4 Q_{cl,0} + C_5 T_d T_o + C_6 Q_{cl,0} T_d + C_7 T_o^2 + C_8 Q_{cl,0} T_o \quad (4.14)$$

$$P_{com,0} = P_1 + P_2 T_o + P_3 T_d + P_4 Q_{cl,0} T_d + P_5 T_o^2 + P_6 T_d Q_{cl,0}^2 + P_7 Q_{cl,0} + P_8 T_o Q_{cl,0}^2 \quad (4.15)$$

$$T_c = a_1 T_d + a_2 T_o + a_3 T_o^2 + a_4 + a_5 T_d T_o + a_6 T_o^3 + a_7 T_d^2 + a_8 T_d T_o^2 \quad (4.16)$$

4.3.3 Compressor Choices

The model contains 15 different options for the compressor in the heat pump. The compressors are operate with different refrigerants and at different temperature levels. The compressors also have different types of regulation. The compressor models and their properties are presented in table 4.4 and the cooling and heating capacity as well as the COP for each model is presented in the diagram in figure 4.12.

Index	Model	Series	Type	Refrig*	To[°C]	Tc[°C]
1	8FE-70Y	Semi-Hermetic	Reciprocating	R134a	-20/11	20/80
2	HSK8591-180	Semi-Hermetic	Screw	R134a	-20/20	20/70
3	CSH95113-320Y	Compact - CSH	Screw	R134a	-45/20	10/60
4	OSK8591-K	Open - OSK(A)	Screw	R134a	-20/20	20/70
5	W6FA-K	Open type	Reciprocating	R717	7/15	10/55
6	OSKA95103-K	Open - OSK(A)	Screw	R717	-20/12	20/65
7	OSHA7452-K	Open - OSHA	Screw	R717	-5/25	18/60
8	OSHA7472-K	Open - OSHA	Screw	R717	-5/25	18/60
9	GSD80485VA	-	Scroll	R410A	8/20	20/65
10	8FE-70Y	Semi-Hermetic	Reciprocating	R404A	-20/7	10/55
11	6F.2Y-K	Open Type	Reciprocating	R404A	-45/8	20/55
12	HSK8591-180	Semi-Hermetic	Screw	R404A	-20/7	10/55
13	OSK8591-K	Open - OSK(A)	Screw	R404A	-20/7	10/55
14	4NSL-30K	Semi-Hermetic	Reciprocating	R744	-50/-15	-20/15
15	6CTE-50K	Semi-Hermetic	Reciprocating	R744	-20/0	5/30

Table 4.4: Properties for compressors obtained from Bitzer, *Reciprocating,**Refrigerant

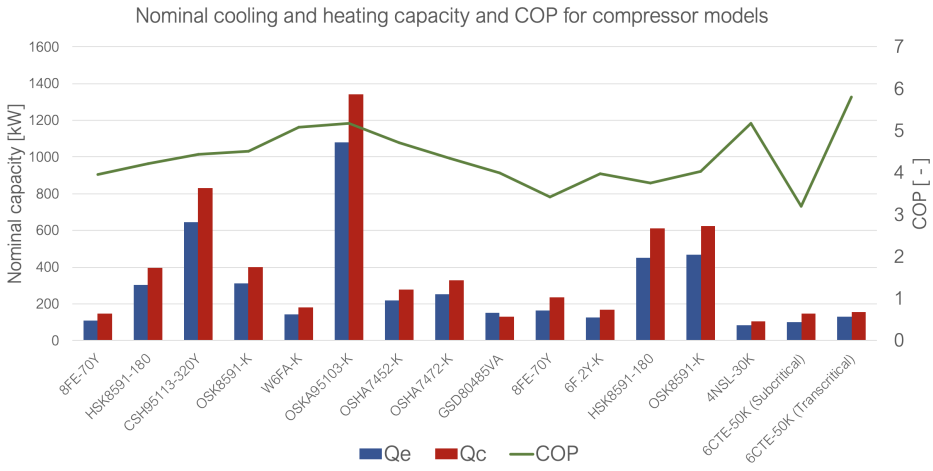

Figure 4.12: Nominal cooling and heating capacity and COP for the compressors specified by the manufacturer Bitzer

4.3.4 Part Load

The part load of the heat pump is a number between zero and one that represent at which load the compressor operate. If the part load is one, the maximum capacity is reached and the heat pump load is at its maximum. If the heating or cooling demand is higher than the capacity a peak load must cover the remaining demand. The part load was calculated for both the condenser and evaporator, then for simultaneity the highest part load was chosen as an overall part load. There are not set any limitations regarding step regulation or a minimum speed for regulation for the part load, so it was assumed that the compressor can operate at any part load between zero and one. Equation 4.17 and 4.18 show how the calculations are performed.

$$pl_h = \frac{Q_{hl}}{Q_{cd}} \quad \text{and} \quad pl_c = \frac{Q_{cl}}{Q_{ev}} \tag{4.17}$$

$$pl = max(pl_h, pl_c) \qquad if\, pl > 1 \quad \rightarrow \quad pl = 1 \tag{4.18}$$

The actual condenser and evaporator loads were calculated by multiplying the capacities with the part load as shown in equation 4.19

$$Q_{cd,real} = Q_{cd} \cdot pl \quad \text{and} \quad Q_{ev,real} = Q_{ev} \cdot pl \tag{4.19}$$

The main result from the heat pump part of the model were the operating condenser, evaporator and compressor power. Figure 4.13 shows a flowchart of the information flow from the BITZER software to the heat pump part of the MATLAB model.

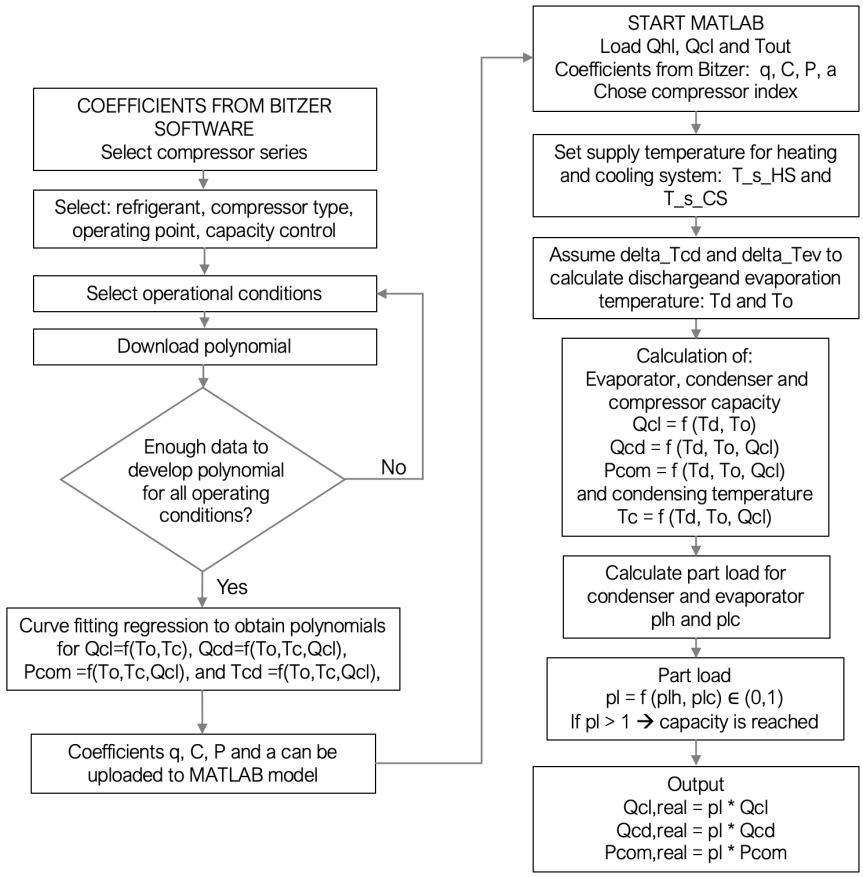

Figure 4.13: Flowchart for BITZER software and heat pump section in MATLAB model

4.3.5 Performance

When the heat pump was not able to cover the heating load, the peak load Q_{peak} cover the remaining load. In the model the peak load lifted the supply temperature in the heating system if the temperature was below 50 °C and it covered the remaining demand when the capacity of the heat pump was reached.

From the calculations of the capacity and real operation of the compressor, condenser and evaporator several performance measures were calculated. The coefficient of performance factor COP, was calculated from the compressor power and condenser heat shown in equation 4.20.

$$COP = \frac{Q_k}{P} \tag{4.20}$$

The seasonal performance factor for the heat pump is the ratio of the total heat output from the condenser and the electricity input to the compressor over a year, equation 4.21.

$$SPF_{HP} = \frac{Q_{HP}}{E_{HP}} \tag{4.21}$$

The total seasonal performance factor of the thermal energy system was also calculated. The total seasonal performance factor of the thermal energy system was calculated by dividing the total thermal energy obtained from heating and cooling from both heat pump and other equipment that cover the total load with the total amount of electricity supplied to operate the equipment. Equation 4.22 shows the calculation.

$$SPF_{tot} = \frac{Q_{heat,HP} + Q_{cooling,HP} + Q_{peak}}{E_{heat,HP} + E_{cooling,HP} + E_{peak}} \tag{4.22}$$

4.4 Modeling of Water Storage Tank

The last sub-model is the water storage tank. The water that is heated by the condenser is transported to the storage tank. In the model it was decided to implement the storage tank layout explained in chapter 2.2 with have three connected pipes; one inflow from the condenser, one outflow to the heating system and one outflow to obtain the mass balance. There is no heat generation inside the tank so the change in energy will be the sum of the flows and losses due to convection.

Table 4.5 presents relevant properties to perform the calculations.

Parameter	**Name**	**Value**	**Unit**
U-value	U	0.22	$\mathrm{W\,m^{-2}\,K^{-1}}$
Temperature of surroundings	$\mathrm{T_{surr}}$	10	°C
Temperature stratification in tank	$\Delta\mathrm{T_{strat}}$	5	°C
Ratio between radius and height	$\frac{\mathrm{r}}{\mathrm{h}}$	$\frac{1}{2.4}$	-

Table 4.5: Thermal properties of the ground

The mass flow of the heating system is dependent on the heating demand. Equation 4.23 show the calculation of mass flow in the heating system in $\mathrm{kg\,s^{-1}}$.

$$\dot{m} = \frac{\dot{Q}}{c_p \cdot \Delta T} \tag{4.23}$$

$\dot{Q}$ = heat delivered to heating system [W]
c_p = specific heat capacity $[\mathrm{J\,kg^{-1}\,K^{-1}}]$
$\Delta T = \mathrm{T_{s,HS}} - \mathrm{T_{r,HS}}$, temperature difference in heating system [K]

For the base case of the model, the water storage tank was sized by assuming a volume for the different loads that are used. The volume was set to be $\mathrm{V_{tank}}$= $100\mathrm{m^3}$. The reason for this is that some issues occur if the volume was too small. The sizing of the buffer tank is a research question that will be further evaluated in chapter 6. The modeling of the thermal energy in the tank was calculated by summation of the in- and outflows in the tank and extract losses due to conduction. The energy balance was presented in equation 4.24.

$$\frac{dE(t)}{dt} = \dot{Q}_{inflow} - \dot{Q}_{outflow} - \dot{Q}_{losses} \tag{4.24}$$

The inflow heat $\dot{\mathrm{Q}}_{\mathrm{inflow}}$ was equal to the heat delivered from the condenser presented in equation 4.25.

$$\dot{Q}_{in} = \dot{Q}_{cd} \tag{4.25}$$

The outflow is the sum of the outflow sent to the heating system and the outflow that directly returns to the condenser. The total heat rate over the heating system was calculated as in equation 4.26.

$$\dot{Q}_{out} = c_p(\dot{m}_{HS} + (\dot{m}_c - \dot{m}_{HS}) \cdot (T_{tank} - T_{s,cond}) = c_p \dot{m}_c \cdot (T_{tank} - T_{s,cond}) \tag{4.26}$$

The heat losses due to conduction are calculated from Fouriers law multiplied with the area of the tank. The area of the cylinder shaped tank can be calculated as in equation 4.27 and the losses as shown in equation 4.28.

$$A_{tank} = A_{top} + A_{bottom} + A_{walls} = 2\pi r^2 + 2\pi rh = 2\pi r(r+h) \tag{4.27}$$

$$\dot{Q}_{losses} = UA(T_{tank} - T_{surr}) \tag{4.28}$$

The energy level can be expressed as shown in equation 4.29.

$$dE = c_p \cdot \rho \cdot V \cdot dT \tag{4.29}$$

$$\frac{dE(t)}{dt} = \dot{Q}_{cd} - c_p \dot{m}_c (T_{tank} - T_{s,cond}) - UA(T_{tank} - T_{surr}) \tag{4.30}$$

$$\frac{dT_{tank}(t)}{dt} = \frac{\dot{Q}_{cd}}{c_p \cdot \rho \cdot V} - \frac{\dot{m}_c (T_{tank} - T_{s,cond})}{\rho \cdot V} - \frac{UA(T_{tank} - T_{surr})}{c_p \cdot \rho \cdot V} \tag{4.31}$$

To obtain the hourly development over time, the equation was temporal discretized, Δt represent the houly time step and i is the current hour. The temperature difference for the steps are calculated as in equation 4.32 and the temperature in the boreholes are calculated as in equation 4.33.

$$\frac{\Delta T_{tank}(i)}{\Delta t} = \frac{\dot{Q}_{cd}(i-1)}{c_p \cdot \rho \cdot V} - \frac{\dot{m}_c(i-1)(T_{tank}(i-1) - T_{s,cond}(i-1))}{\rho \cdot V} - \frac{UA(T_{tank}(i-1) - T_{surr})}{c_p \cdot \rho \cdot V} \quad (4.32)$$

$$T_{tank}(i) = T_{tank}(i-1) + \Delta T_{tank}(i) \quad (4.33)$$

Figure 4.14 shows the flow chart of the water tank sub-model.

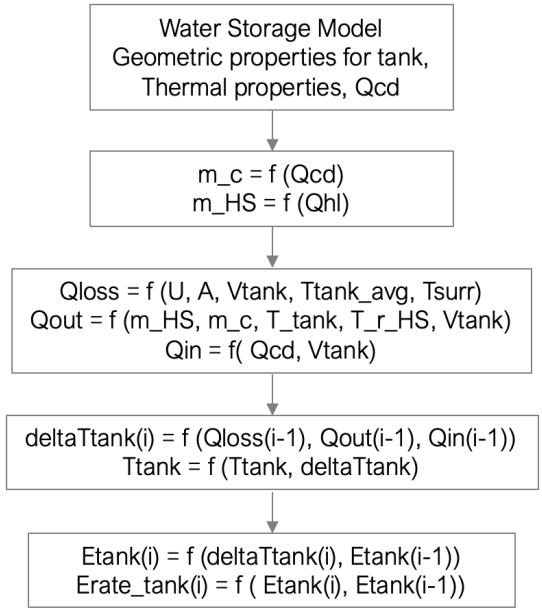

Figure 4.14: Flowchart water storage tank

4.5 Overview of Assumptions That are Made

A lot of assumptions and simplifications are performed to carry out the model. This section presents an overview of these assumptions and simplifications.

1. *Heat loss in pipes and in heat exchangers are neglected.* Ideal heat transfer and heat transport between components.
2. *No limitations for compressor operation.* Variable speed drive from 0-100 %.
3. *Simplified water storage tank.*
    a. Thermal stratification of the tank is not calculated but assumed, the height of the tank is not taken into account.
    b. Independent operation of water storage and heating system is not implemented.
    c. Heat rates are calculated rather than flow rates
4. *Geothermal properties.* Geothermal properties are assumed from typical or average values in Norway. Must be known for the actual location to be interpreted in actual system.
5. *All heating and cooling demand for building or area are combined to one load.* No distinguishing between domestic hot water and space heating or space cooling and process cooling.
6. *Inflows and outflows for each borehole is combined to one large inflow and outflow.*
7. *The temperature of the outflow of the borehole storage is equal to the temperature in the borehole storage.*

Results of Base Case Model with Two Heating and Cooling Loads

In this section results from the base case of the model is presented. The model was tested with two particular loads and the results are used to validate the model. The chapter is wrapped up by remarking some issues with the results.

5.1 The Loads Used in the Model

The model is tested with two main base loads, these are presented in this section. The two loads consist of an hourly heating and cooling demand. The first load have a relatively high and constant heating and cooling demand throughout the year, this load is named Load 1. The other load have larger seasonal differences in the demand, this load is named Load 2. The purpose of using two loads is to compare if some solutions work better for one load type than the other.

5.1.1 Load 1 - Constant and Large Heating and Cooling Demand

Load 1 consist of a large heating and cooling demand. The heating demand is relatively constant over the year with a small increase in demand during the winter months. The cooling demand is constant over the year and there are no seasonal differences. There are simultaneous heating and cooling demand so that the condenser and evaporator both supply their corresponding heating and cooling system. Table 5.1 present key information for the load and figure 5.1,5.5 and 5.3 shows the hourly heating and cooling demand for a year, the monthly heating and cooling demand and the duration curve for Load 1.

Demand	Maximum [kW]	Total [MWh]
Q_{hl}	2768	6436
Q_{cl}	1015	3386
Ratio (Q_{cl}/Q_{hl})	-	0.53 [-]

Table 5.1: Maximum and total heating and cooling demand for Load 1

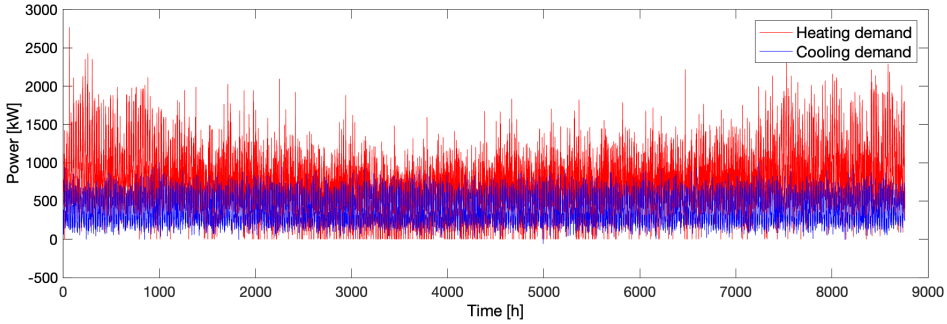

Figure 5.1: Hourly heating and cooling demand for Load 1

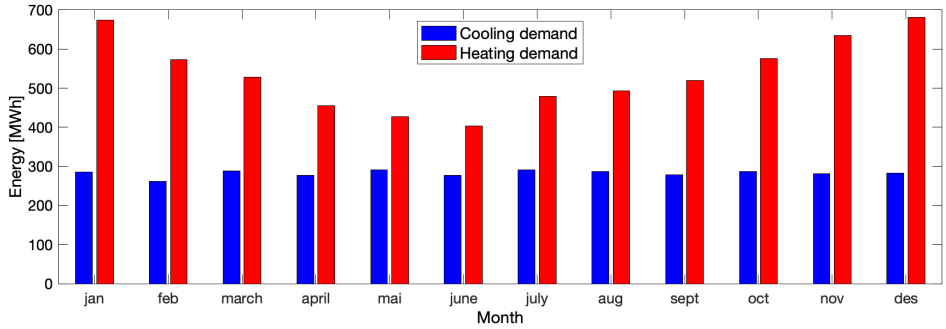

Figure 5.2: Monthly heating and cooling demand for load 1

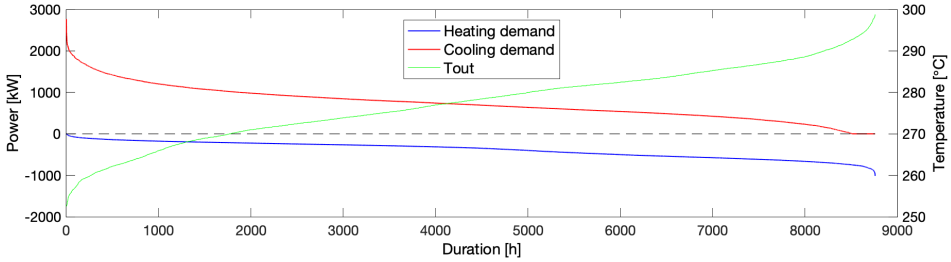

Figure 5.3: Duration curve for Load 1

5.1.2 Load 2 - Heating and Cooling Demand with Seasonal Differences

Load 2 originally consist of a smaller heating and cooling demand. Both the heating and the cooling demand have large seasonal differences and the demands are not overlapping. This means that if there is a heating demand, there is no cooling demand. Table 5.2 present key information for the load and figure 5.4 shows the hourly heating and cooling demand for a year. Monthly demand is presented in figure 5.2. The maximum cooling demand is much higher than the maximum heating demand, but the monthly demand shows that the total cooling demand during the summer is lower than the heating demand during winter months. The high cooling demand is only for short periods of time. Figure 5.6 presents the duration curve for Load 2.

Demand	**Maximum [kW]**	**Total [MWh]**
Q_{hl}	334.7	1073.4
Q_{cl}	832.5	316.2
Ratio (cl/hl)	-	0.29 [-]

Table 5.2: Maximum and total heating and cooling demand for Load 2

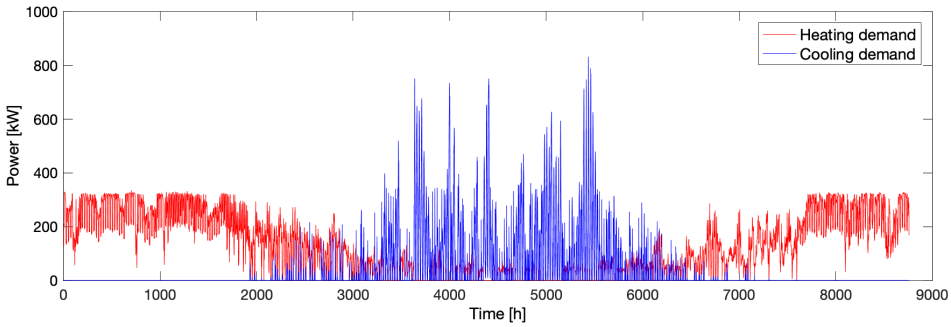

Figure 5.4: Hourly heating and cooling demand for load 2

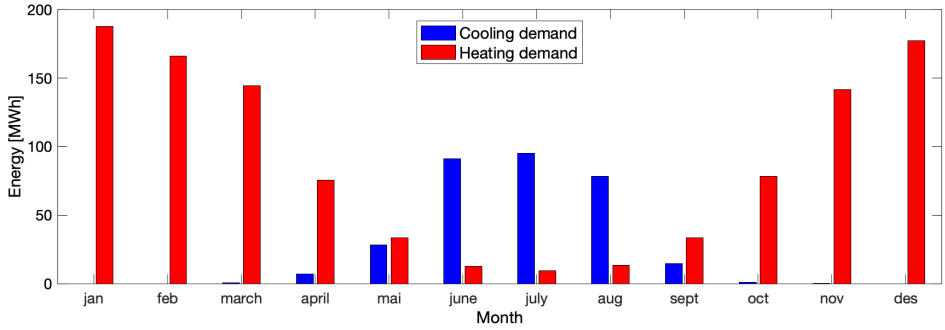

Figure 5.5: Monthly heating and cooling demand for load 2

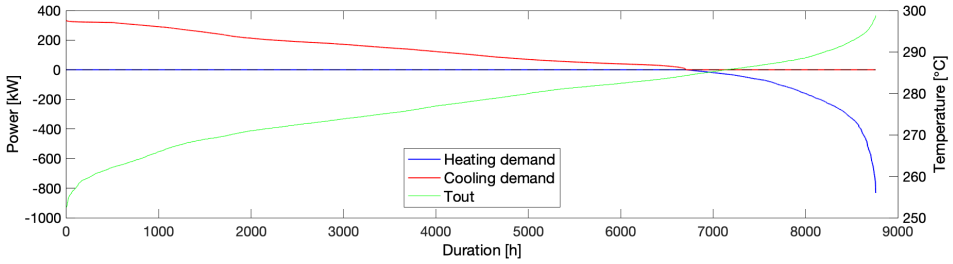

Figure 5.6: Duration curve for Load 2

The duration curves for Load 1 and Load 2 are presented in figure 5.3 and 5.6.

While Load 1 have a moderate slope for both heating and cooling demand, Load 2 have an exponential slope for the cooling demand. The duration curve demonstrate that the heating and cooling demand are never overlapping for Load 2, when the heating demand is larger than zero, the cooling demand is zero, and opposite.

5.2 Results From the Basecase for Load 1 and Load 2

Load 1 and Load 2 is run with the basecase model presented in chapter 4.

5.2.1 Basecase for Load 1

The basecase model is tested for Load 1. The base case of the model include demand control for borehole storage and the water storage tank. For Load 1 compressor number 6 is used. Compressor number 6 is an open screw compressor using Ammonia as refrigerant and have a maximum condenser capacity of 1340 kW. The condenser capacity is approximately 50 % of the maximum demand.

Parameter	**Name**	**Value**	**Unit**
Energy delivered to heating system	Q_{hs}	6549	MWh
Energy delivered to cooling system	Q_{cs}	6076	MWh
Heat covered by heat pump	Q_{hp}	6161	MWh
Heat covered by peak load	Q_{peak}	388	MWh
Average compressor capacity	P_{comp}	112	kW
Average condenser capacity	P_{cond}	1221	kW
Average evaporator capacity	P_{evap}	1109	kW
Seasonal Performance Factor	SPF	10.9	-
Carnot, Seasonal Performance Factor	SPF_{carnot}	15.7	-
Maximum/minimum temperature in boreholes	$T_{bh,max}$	7.1/5.9	°C
Average temperature in boreholes	$T_{bh,max}$	6.5	°C
Maximum/minimum temperature in storage tank	$T_{bh,min}$	55.4/40.9	°C
Average temperature in storage tank	$T_{bh,max}$	51.8	°C

Table 5.3: Main results from Basecase with Load 1

Figure 5.7 presents the temperature, energy level, heat rate and cumulative heat rate in the boreholes.

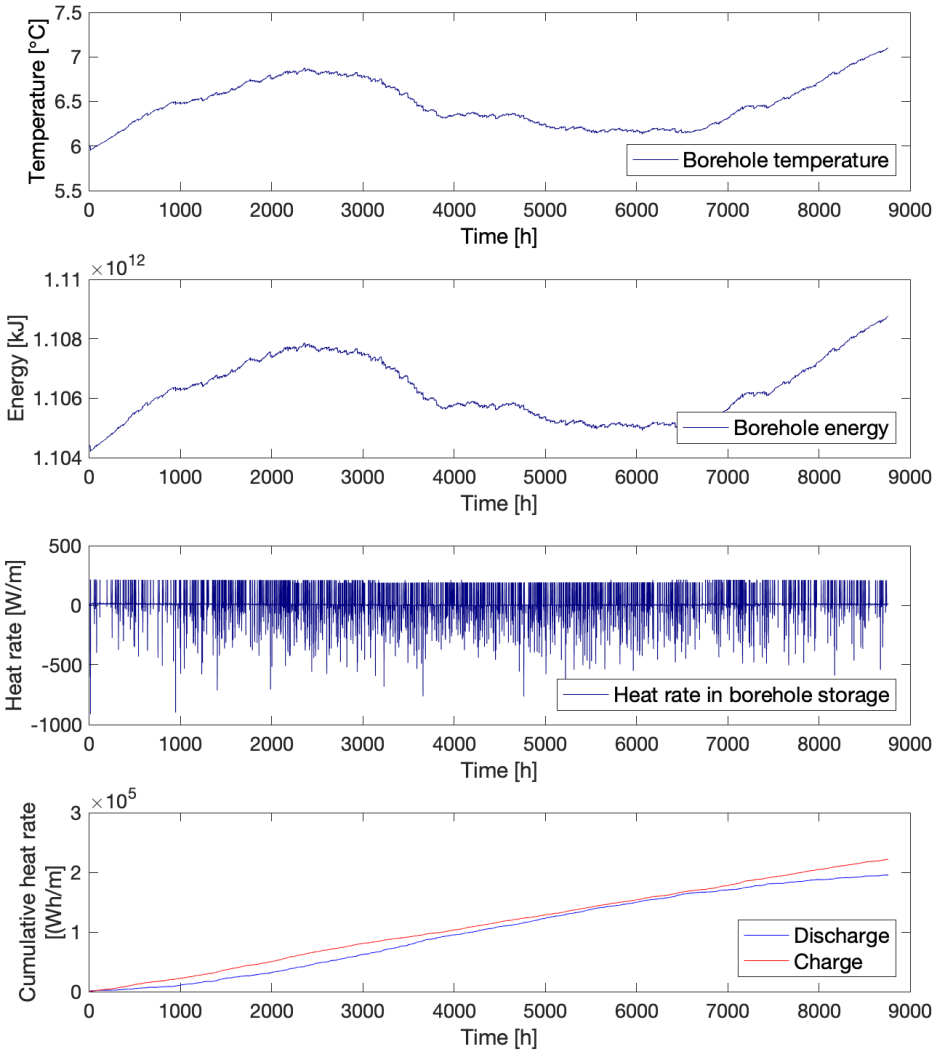

Figure 5.7: Load 1: Temperature level, energy level, heat rate and cumulative charge and discharge in borehole storage

The last diagram in figure 5.7 shows a cumulative graph of the charging and discharging in the borehole storage. When the charge curve is steeper than the discharge curve the temperature increases and the discharge curve is the temperature decreases. The slope of the charging and discharging curves have been calculated for four time steps over the year. The time steps have been chosen graphically from where the slope seems to change steepness. The result of the calculations are presented in table 5.4. The rates are a bit higher than the heat rate of the ground which usually is 30-40 $\mathrm{W\,m^{-1}}$, but the values are still within reasonable values (NGU 2020a).

Time step [h]	**0:2000**	**2001:6500**	**6501:8760**
Slope Charge [W/m]	52.5	47.1	56.6
Slope Discharge [W/m]	41.0	58.0	39.8

Table 5.4: Load 1: Slope of charging and discharging the boreholes.

The temperature level, energy level, heat rate and cumulative charging and discharging in the tank is presented in figure 5.8. The reduction in temperature from during summer season is due to the reduced set point temperature for the heat pump when the outdoor temperature exceed 7 °C. The temperature and energy level in the water storage have a much faster response time, which is expected from the short term energy storage.

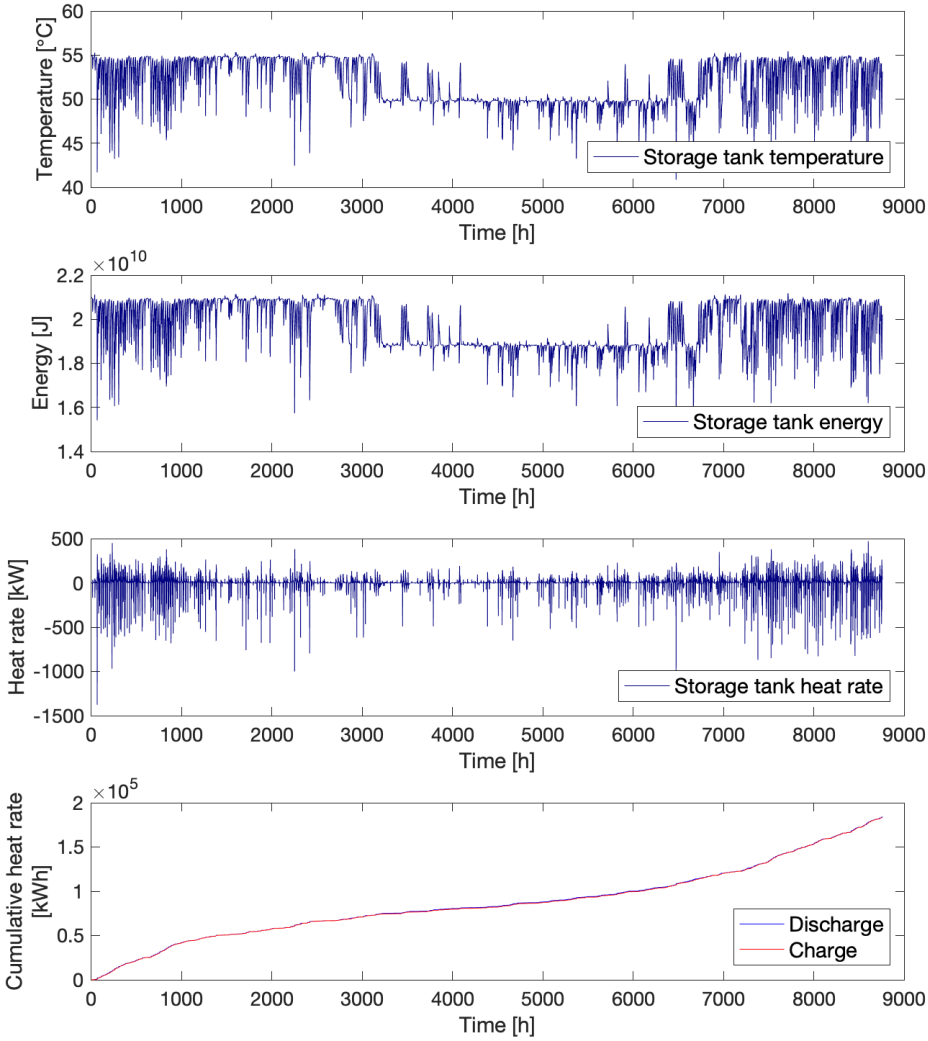

Figure 5.8: Load 1: Temperature level, energy level, heat rate and cumulative charge and discharge in water storage tank

A cumulative charging and discharging graph is also made for the water storage tank, this is presented in figure. The charging and discharging of the tank follow each other quite close which indicate that the flows in the tank are in balance.

The temperature level in the heating system is presented in figure 5.9. If the temperature in the buffer tank is below 50 °C it will be lifted by the peak load. The return temperature in the cooling system is calculated from a constant mass flow and there is therefore more variation than for the other temperatures.

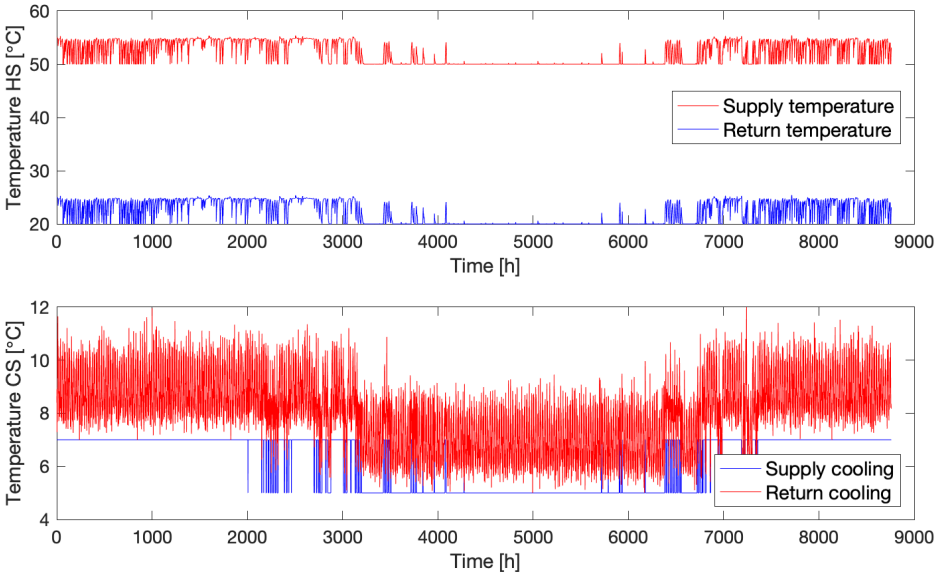

Figure 5.9: Load 1: Temperature heating system

The peak load will lift the supply temperature to the heating system when needed, and it will also cover the heating demand that exceeds the heat pump capacity. Figure 5.10 shows the heat delivered from the heat pump and from the peak load over the year. Figure 5.11 shows the monthly demand covered by the peak load in relation to the demand covered by the heat pump.

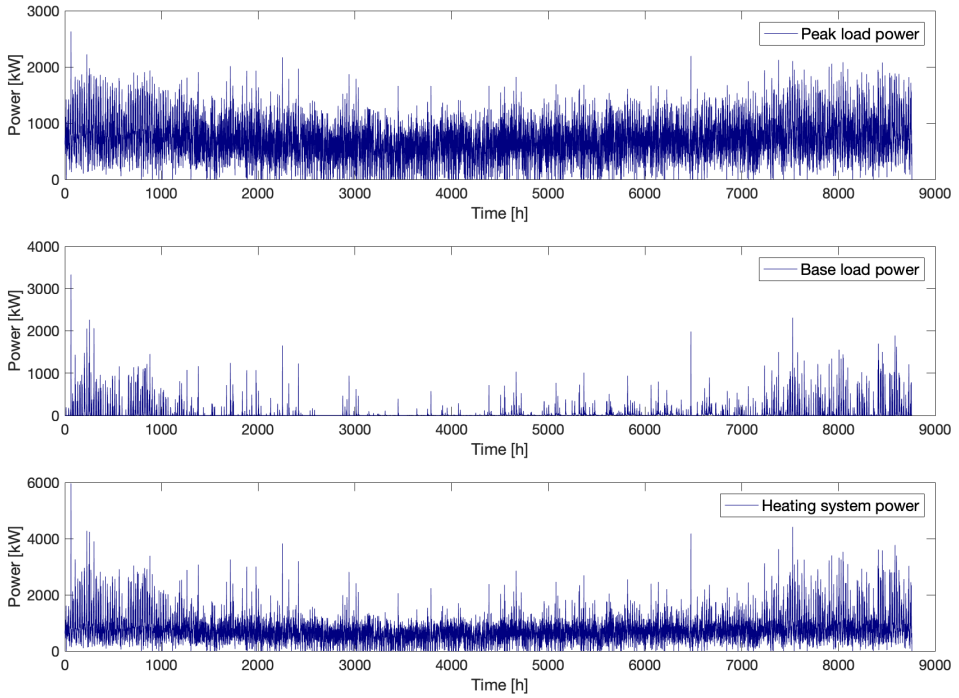

Figure 5.10: Load 1: The heat delivered from the base load and the peak load and the total heating system

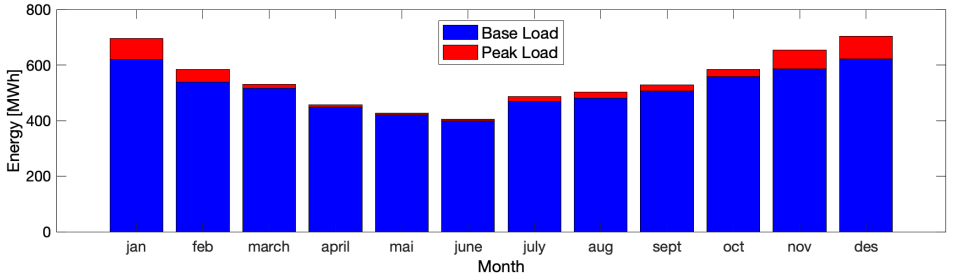

Figure 5.11: Load 1: The coverage of the base load and the peak load, the base load in this case is the heat pump.

It can be observed that the total heating system sometimes deliver more heat than demanded, but usually the heating system is equal to the heating demand.

Figure 5.12 shows the frequency of part load for the system.

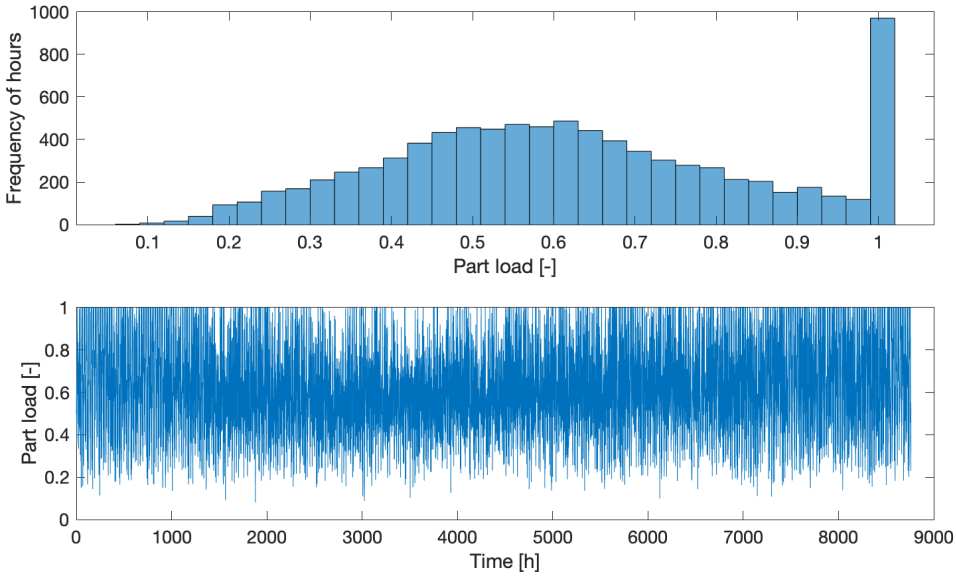

Figure 5.12: Load 1: Part load frequency

The heat pump is running at full capacity almost 1000 hours over the yeas, from the lowest graph it can be seen that the is more often on full capacity during the winter months.

5.2.2 Basecase for Load 2

The results from testing the basecase model with Load 2 is presented in this section. For Load 2 the compressor model is 8FE-70Y which is a Semi-Hermetic Reciprocating compressor. The compressor have a condenser capacity of 234 kW and uses R404A as refrigerant. Table 5.5 present the main result for the thermal energy system with Load 2.

Parameter	**Name**	**Value**	**Unit**
Energy delivered to heating system	Q_{hs}	1058	MWh
Energy delivered to cooling system	Q_{cs}	1101	MWh
Heat covered by heat pump	Q_{hp}	1003	MWh
Heat covered by peak load	Q_{peak}	55	MWh
Average compressor power	P_{comp}	44.9	kW
Average condenser power	P_{cond}	271.8	kW
Average compressor power	P_{evap}	228.1	kW
Seasonal Performance Factor	SPF	6.1	-
Carnot, Seasonal Performance Factor	SPF_{carnot}	12.8	-
Maximum/minimum temperature in boreholes	$T_{bh,max}$	10.6/6	°C
Average temperature in boreholes	$T_{bh,avg}$	8.5	°C
Maximum/minimum temperature in storage tank	$T_{bh,max}$	55/40.2	°C
Average temperature in storage tank	$T_{bh,avg}$	50.2	°C

Table 5.5: Main results from Basecase with Load 2

The temperature level, energy level, heat rate and cumulative charging and discharging of the tank in the borehole storage is shown in figure 5.13. It can be seen that there are seasonal temperature differences and that the borehole storage respond as desired and is charged during summer season.

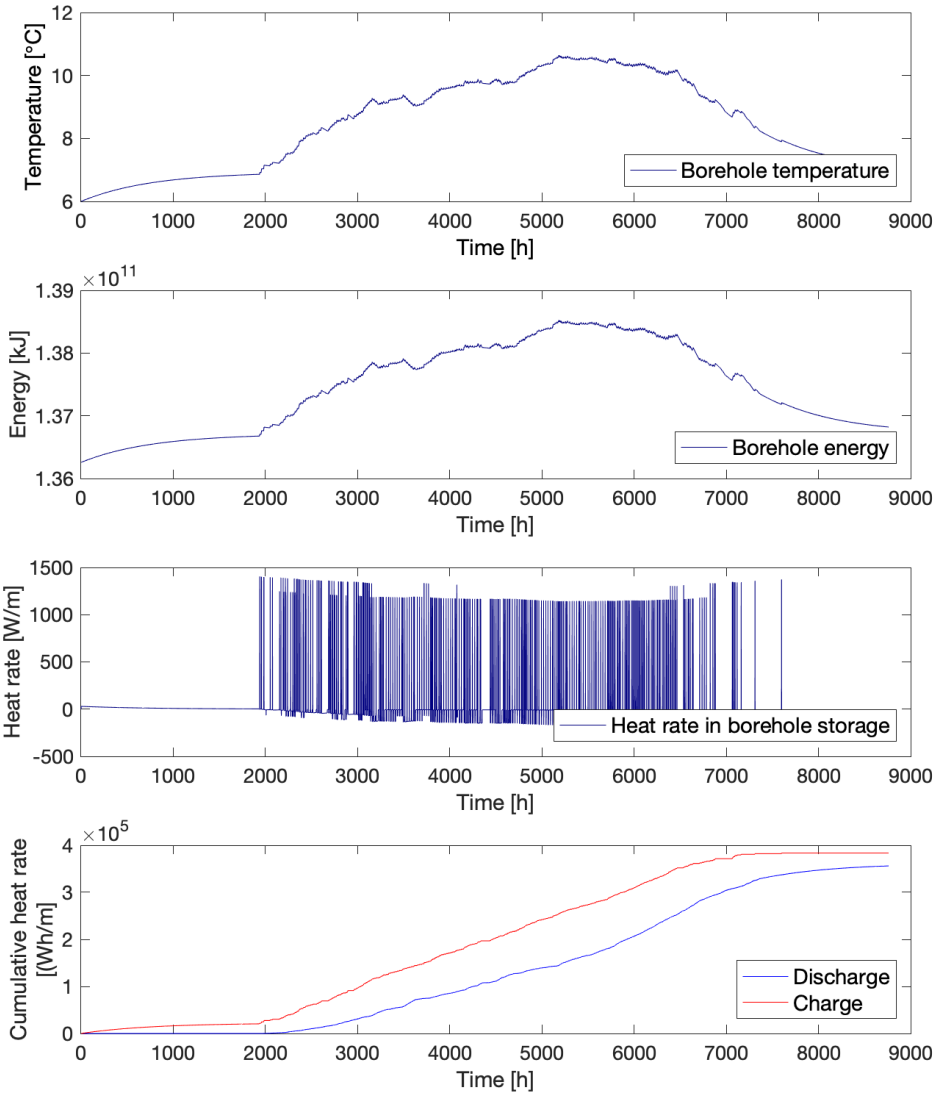

Figure 5.13: Load 2: The temperature level, energy level, heat rate and cumulative charging and discharging of the tank in the borehole storage

The heat rate in the borehole storage is presented in figure. The positive heat rate is the head delivered to the boreholes and the negative heat rate is the

heat extracted from the boreholes. The last graph in figure 5.13 presents a cumulative graph of the charging and discharging. The slope of the charging and discharging is almost zero until t = 2000h, then both increase until t = 7000h then, the slope for both is decreasing towards zero. The slope of the charging curve from t = 2000:7000 is 70 W/m and for the discharge curve 60 W/m, the values are a bit high compared to the values presented by NGU (2020a).

The water storage tank work as a short term storage, the temperature level, energy level, heat rate and cumulative charge and discharge of the tank is presented in figure 5.14. From the temperature and energy levels it can be observed that the temperature in the tank is decreasing for a longer period of time. The cumulative graph indicate that the discharging of the tank is larger during summer season. This indicate that the storage tank might be too large, the sizing of the tank will be further evaluated in the research questions.

The heat rate of the water storage tank is presented as the third graph in figure 5.14. The positive heat rate is the heat delivered to the tank and the negative heat rate is the heat extracted from the tank.

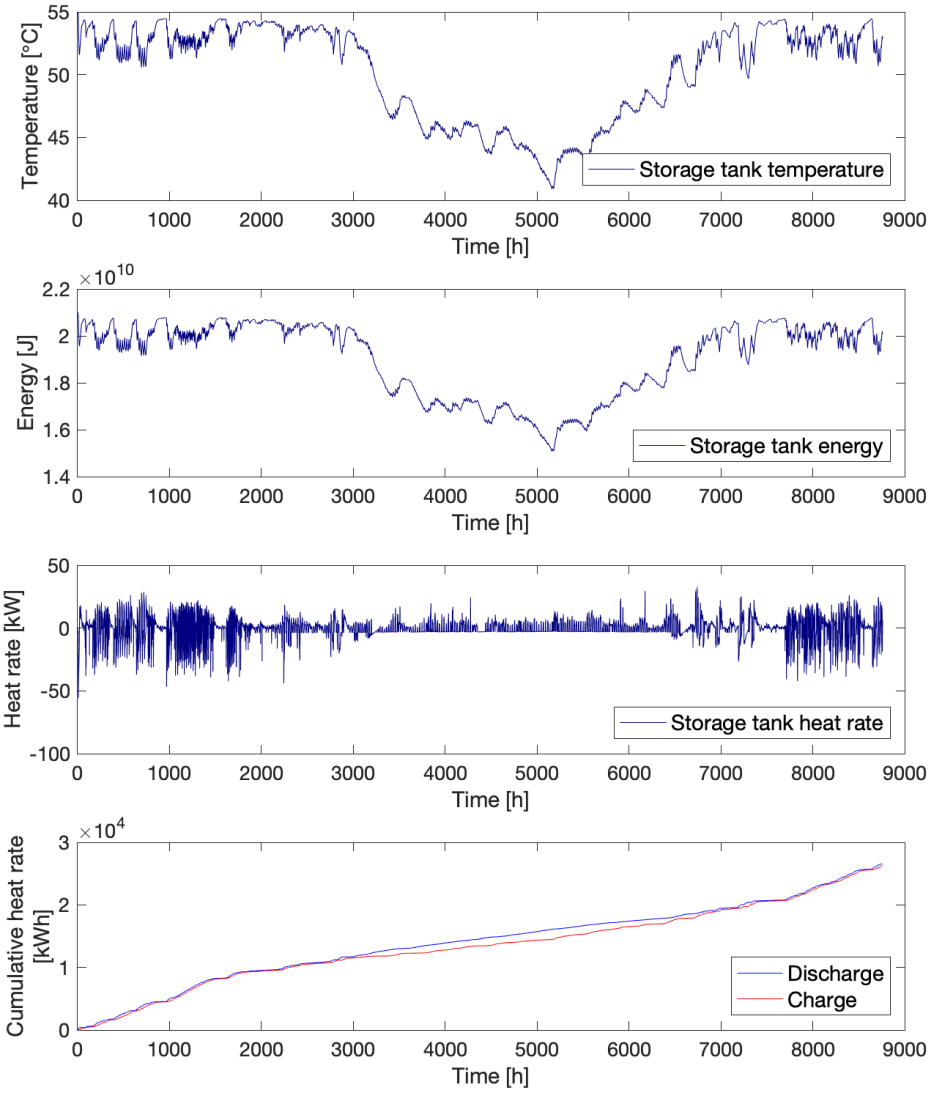

Figure 5.14: Load 2: Temperature, energy, heat rate and cumulative charge and discharge in water storage tank

The supply temperature in the heating system is assumed to be equal to the tank temperature, unless the tank temperature is below 50 °C, then the temperature

is lifted by the peak load. The temperature level in the heating system can be seen in the upper figure 5.15. The return temperature is 30 °C lower than the supply temperature.

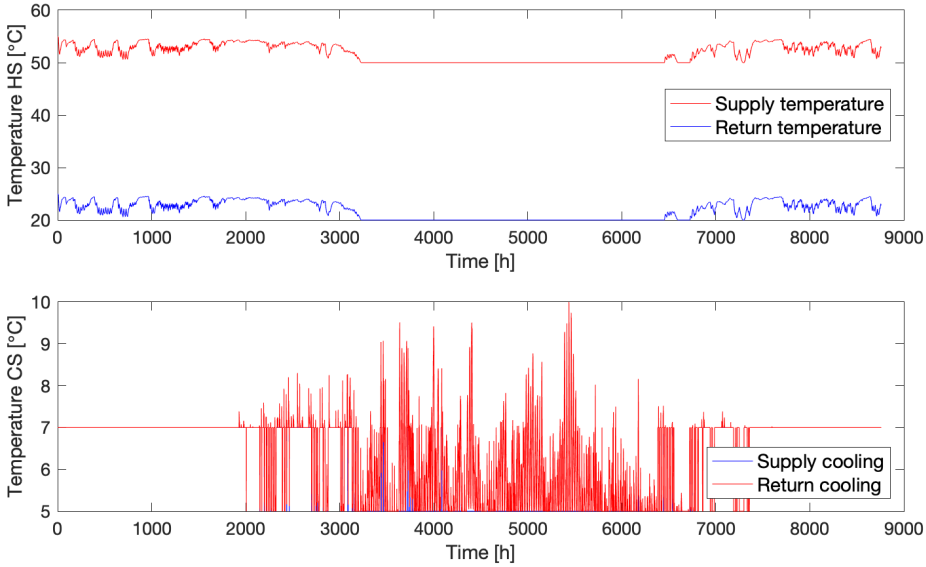

Figure 5.15: Load 2: Temperature heating system

The demand for peak load to cover remaining heat demand after the heat pump is presented in figure 5.16. The demand for extra heat to cover the total demand is mainly during winter season.

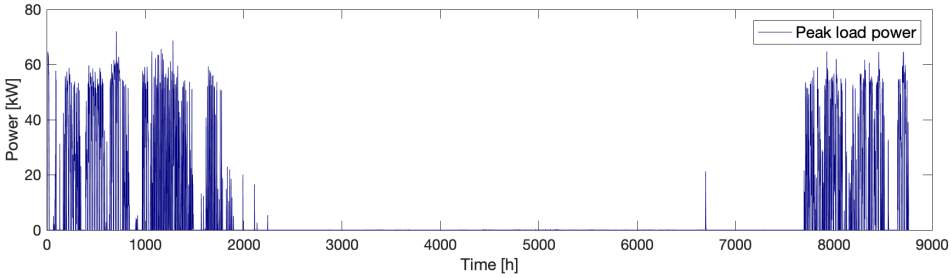

Figure 5.16: Load 2: Peak load demand

The frequency of the part load is presented in figure 5.17.

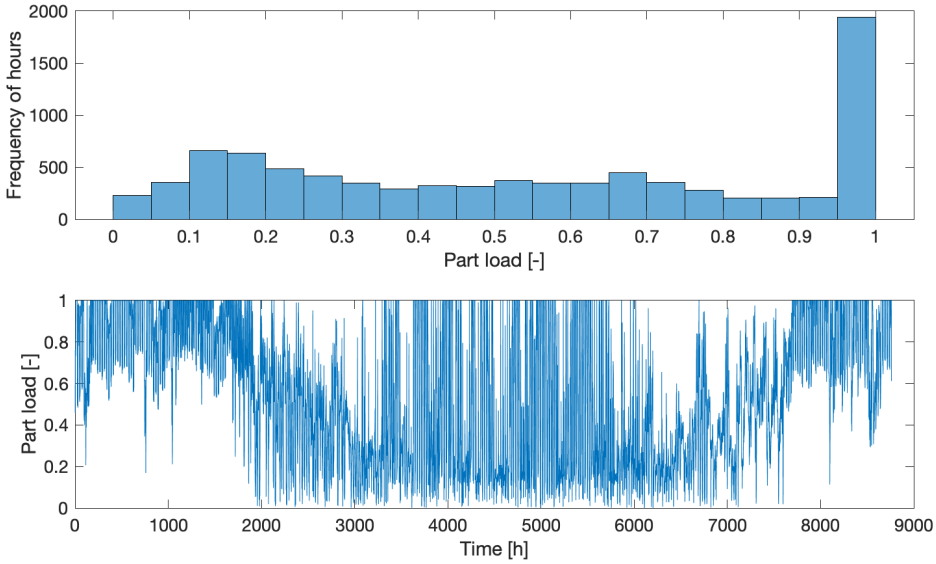

Figure 5.17: Load 2: Part load frequency

5.2.3 Remarks

There are some remarks to be made for the results presented for the base case for Load 1 and Load 2.

- Seasonal temperature development in boreholes for Load 1 is not responding as desired, the temperature increases during the first quarter of the year, then in the second and third quarter of the year the temperature is decreasing before it increases in the last quarter.
- High COP, due to low compressor capacity. Even if the evaporator and condenser capacity is maximized, the compressor load is lower than the capacity.
- The short term water storage tanks thermal energy storage are within reasonable limits regarding the temperature and energy balance. The charging and discharging follow each other. But for Load 2 the temperature in the storage tank decreases for a longer period.
- The peak load power is frequently very high for Load 1.

Research Questions in Model

In this chapter, research questions in the model are presented for further analysis and discussion. The purpose is to identify and understand how such an integrated plant will work and perform under different conditions. The research questions include improvements in the model and testing of common issues in thermal energy systems with heat pumps. Research questions regarding the model and how assumptions and simplifications affect the results are evaluated, as well as research questions regarding the system's performance regarding various loads, methods for sizing, temperature levels, choices for the compressor, and control solutions.

6.1 Influence of Various Loads in Model

Variation in the heating and cooling load is tested in the model to see how the system responds to different loads. For the SWECO building in Bergen, the actual cooling demand was 70 % lower that the pre-calculated demand (Aaberg 2019), this results in a possibility of supercooled borehole storage over time. Variation in the load can influence the performance of a ground-source heat pump system using the borehole configuration as a seasonal thermal energy storage. The heating and cooling load is calculated in advance and used to size the thermal energy system. For this reason, the deviation between pre-calculated and actual heating and cooling demand will result in a thermal energy system that is poorly dimensioned. If the thermal energy demand is smaller or higher than the pre-calculated demand, this can result in poor performance of the system and an unbalanced seasonal thermal energy storage that will become supercooled with time. For this section, an analysis of the loads is performed in Energy Earth Designer to compare the temperature development with the result in the model and to evaluate the consequences of deviation in the actual loads compared to the pre-calculated loads. By changing the heating and cooling loads and their ratio and perform a simulation under the same

conditions in Energy Earth Designer, it would be possible to estimate the long term storage sizing and operation.

6.1.1 Energy Ratio Between Heating and Cooling Demand

Load 1 and Load 2 are scaled and changed to test the model with different loads. In Load 1 and Load 2, the yearly cooling and heating demand ratio is approximately 0.53 for Load 1 and 0.29 for Load 2. The loads are scaled and changed to test the model and EED with different loads and ratios. The main goal is to evaluate the influence of the various loads in the borehole storage. The test ratios are presented in table 7.4.

Load	Change in Qcl	Ratio	Load	Change in Qcl	Ratio
Load 1	Base Case	0.53	Load 2	Base Case	0.29
Load 1	-50%	0.26	Load 2	+50%	0.44
Load 1	+50%	0.79	Load 2	+150%	0.74

Table 6.1: Energy ratio of cooling and heating demand tested in model and in Energy Earth Designer

6.1.2 Energy Earth Designer

Energy Earth Designer can be used to check the temperature in the borehole storage over time. This is executed by implementing the same ground properties, borehole configuration, properties of the brine and the monthly energy values for base and peak load. The input values used to test the borehole storage can be found in the Appendix A.7. The main goal of using Energy Earth Designer is to test the energy balance in the borehole storage over time. If the extracted heat is much higher than the heat delivered to the boreholes there is a risk of cooling down the borehole storage over time. If the temperature become too low there is a risk of freezing the brine and for the temperature lift for the compressor to become large. If the temperature lift in the compressor is too large, this can result in higher wear on the compressor and at worst a compressor breakdown. The purpose of testing the loads in EED is to compare the results from the software with the results from the model.

6.2 Sizing the Thermal Energy Storages

The integrated thermal energy system consists of two thermal energy storage. The borehole storage is a seasonal thermal energy storage that is thermally charged during the summer season and thermally discharged during the winter season. The water storage tank between the condenser and the heating system is a short-term storage with an hourly perspective on charging and discharging heat. The sizing of these systems is essential to the operation of the integrated thermal energy system. This section presents solutions for sizing the thermal energy storage that was tested in the model.

6.2.1 Sizing the Short-Term Water Storage Tank

In the base-case, the volume of the water storage tank is sized from assuming a volume. This solution was chosen for simplicity. As presented in chapter 2.2, there are several solutions for sizing a water tank storage. It was tested to size the heat pump using the minimum part load capacity method and the residence time method. The methods are presented in respectively equation 6.1 and 6.2.

$$V_{storage,tank} = p_{\text{Qk,min}} \cdot Q_k \cdot V_{specific} \tag{6.1}$$

where:

$p_{\text{Qk,min}}$ = Minimum Performance Step [%]
Q_k = Condenser Capacity of Heat Pump [kW]
$V_{specific}$ = Specific Volume [$1\,kW^{-1}$]

$$V_{storage,tank} = \tau \cdot \dot{m} \tag{6.2}$$

where:

τ = residence time [h]
V = volume of the tank [m^3]
$\dot{m}$ = nominal mass flow supplied to the heating system [m^3/h]

For the minimum part load capacity method the following minimum part load capacity and residence time was tested in the model. It is expected that the model have more rapid response as the tank become smaller.

Min Performance Step:	20 %	30 %	40 %	50 %	-	-
Residence Time τ:	30 min	1 h	1.5h	2 h	3h	4h

6.2.2 Sizing the Seasonal Borehole Storage

The sizing of the boreholes in the model is presented in section 4.2.1. The sizing involves simplifications and assumptions. When the model is run, it can be observed that the temperature differences in the borehole storage are limited compared to the temperature differences by running the system in the Energy Earth Designer. One reason for this can be the enormous volume calculated as the volume of the borehole configuration. Another reason can be that the mass flows of the brine in each borehole are merged into one large flow in the model. This simplification of the boreholes will probably affect the temperature distribution on the borehole configuration. It is tested if reducing the total volume will have an impact on the temperature differences. The total volume of the borehole storage is increased and reduced to observe the impact on the temperature difference. It is predicted that reducing the volume of the borehole configuration will increase the seasonal temperature difference in the storage.

6.3 Influence of Temperature Levels

Temperature levels in a thermal energy system is essential to its performance and efficiency. Otto Nielsens Vei 12 E delivered surplus heat to the neighbor building at high temperature levels and this results in a reduced amount of delivered energy and reduced performance of the heat pump (Alfstad 2018). In this section particular temperature levels in the system are evaluated. The return temperature from the evaporator and condenser are input values in the model, and can be changed within some limits.

6.3.1 Temperature Level for Heating System

In the base case model, the heating system's temperature level is set to change between two set-point temperatures depending on the outdoor temperature. The model is tested with a second strategy for the temperature level of the condenser's secondary side. The first strategy is to increase the temperature by decreasing outdoor temperature. The relation between the supply temperature and the outdoor temperature is obtained from measurements from two heat pumps at NTNU obtained from the facility operator NTNU drift. A curve fitting regression is performed on the measurements to generate the relation. The relation between the outdoor temperature and the temperature in the heating system is presented in figure 6.1, and the temperature level using this temperature strategy during the year is presented in figure 6.2.

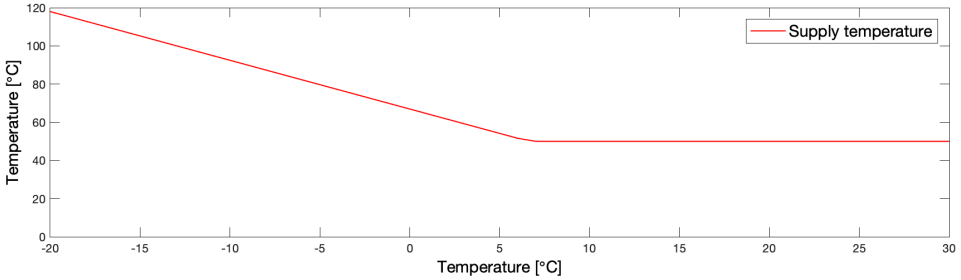

Figure 6.1: Temperature from Heat Pump relative to outdoor temperature

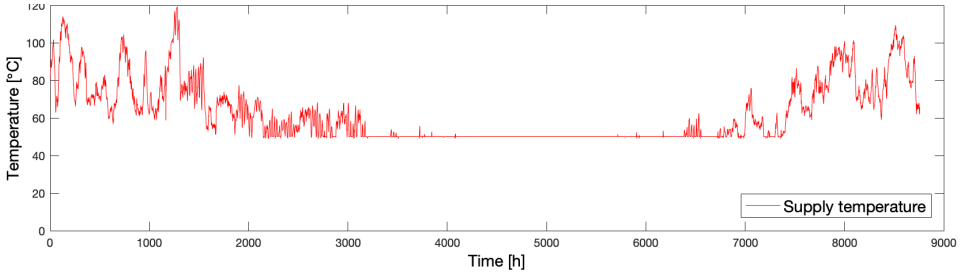

Figure 6.2: Hourly temperature from Heat Pump over a year

This strategy will be tested and compared to the strategy in the base case. Note

that using these temperature levels will for some time over the year exceed the heat pump capacity for the condenser temperature.

The strategy used in the base case for choosing the return temperature for the secondary side of the condenser is to use a higher temperature when it is cold, and a lower temperature when it is warmer, in the model it is tested to use 55°C when T_{out} is lower than 7 °C and 50 °C if T_{out} is higher than 7 °C. Over a year this will result in the following temperature from the condenser presented in figure 6.3.

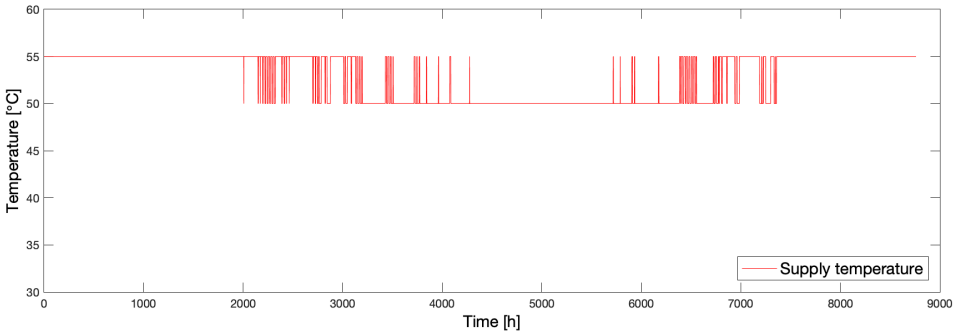

Figure 6.3: Hourly temperature from Heat Pump relative to outdoor temperature

Return Temperature in Heating System

The return temperature in a heating system is essential to the performance of a heat pump. An issue that frequently occur is that the return temperature to the condenser is too high. This results in inadequate performance for the heating system. The return temperature in the model is either set to be the supply temperature minus an assumed temperature difference or is calculated due to an assumed mass flow. The goal was to test the influence of the performance due to the return temperature, but since the performance polynomials are not a function of the return temperature this was not possible.

6.3.2 Temperature Level for Cooling System and Its Influence On the Borehole Temperature

The return temperature on the secondary side of the evaporator is set to be 7 °C when the outdoor temperature is lower than 7 °C and 5 °C when the outdoor temperature is higher than 7 °C. The return temperature from the evaporator is equal to the temperature supplied to the cooling system $T_{s,CS}$. This results in a return temperature $T_{r,CS}$ from the cooling system that is quite high, as presented in chapter 5. From the base case in chapter 5 for Load 1 it can be observed that the temperature in the boreholes do not respond as desired. The seasonal temperature differences are low and the temperature is decreasing during summer season. It is tested if reducing the temperature in the cooling system with 4 °C will have a impact on the response. The expectation is that the temperature in the borehole storage will increase during summer also for Load 1. For Load 2 it is assumed that the temperature difference will increase.

6.4 Choice of compressor for Heat Pump

The various compressors for the heat pump vary in capacity and COP. The compressors must be evaluated to find the best match for the thermal energy system that it will operate in. The size, refrigerant and efficiency of the heat pump can be used to make a choice. Different compressor models are tested for the model to analyze which compressor have the best overall performance in the thermal energy system. Since the heat pump capacities in the model only depend on the set-point condenser and evaporator temperatures. The test is performed with the evaporator and condenser temperature from the base case model. For some of the compressor the set-point temperatures are outside of their operating temperature range. How this affect the performance will be evaluated in the results.

Compressor CSH95113-320Y is tested with different temperature levels in its operating range to see how the temperatures and the temperature lift impact the performance. This compressor have a wide range of operating temperatures for both the condenser and evaporator. The temperatures presented in table 7.5 are tested. For simplicity the temperature is kept constant over the year and is not change due to outdoor temperature.

Temperature lift	$\mathbf{T_{r,cond}/T_{r,evap}}$	**Unit**
Base Case	55/5	°C
+10	60/0	°C
-10	50/10	°C

Table 6.2: Change in temperature lift to influence the performance

6.5 Control of the thermal energy storage

There are two thermal energy storages in the model. One short-term energy storage and one seasonal storage. In this section the various control solutions are presented for further testing.

6.5.1 Control of Water Storage Tank

The water storage tank is a short-term energy storage. In the base case model the buffer tank was demand controlled. This means that in free cooling mode there are no heat supplied to the tank from the condenser. From chapter 5 it can be seen that the borehole temperature for both loads are within reasonable limits, but for Load 2 there is a long term decrease in temperature and energy level. There are several solutions for control of a water storage tank. Some tanks do not have control at all, and the tank is only damping the largest disturbances. Other tanks are controlled to enable independent operation of the tank and the heating system. The model is tested with no control strategy to observe how such a strategy differ from the demand controlled tank.

6.5.2 Control of Boreholes

Two control strategies are tested for the seasonal thermal energy borehole storage. The first strategy is the strategy used in the base case control of the system considering the heating and cooling demand. The second strategy is control based on season. Control on demand is implemented by using an if-sentence with conditions associated with different operational modes. The conditions are presented in table 6.3.

Operational mode	Condition for if-sentence
Overall heating mode	if Q_{hl}>Q_{cl}
Overall cooling mode	if Q_{cl}>Q_{hl}
Free cooling mode	if Q_{cl}>0 && Q_{hl}==0

Table 6.3: Conditions to control system in particular operational modes

Control on season is obtained by shifting the control of the system during the season. In the model this is obtained by using a for loop for each season with change in operational conditions. The particular for loop for each operational mode contains the relevant heat rates for mode the during the relevant period. The for loops shift to overall cooling mode during summer months and then shift back to overall heating when the summer is over.

6.6 Sensitivity Analysis of Uncertain Input Data in the Model

The thermal energy system consist of many assumptions and simplifications that causes uncertainties in the model. In this section a sensitivity analysis will be performed in order to evaluate the influence of uncertain components in the model.

6.6.1 Influence of BITZER Coefficients

The coefficients obtained from BITZER are an element of uncertainty in the model. It is not easy to control their validity without performing measurements on a thermal energy system with an integrated compressor from BITZER. As the coefficients are delivered from the manufacturer there is a possibility that the coefficients deliberately provide very good performance for the system. The model is tested with increasing and decreasing the coefficients by 10 %.

q, C, P, a	$+/-$ 0 %
q, C, P, a	$+$ 10 %
q, C, P, a	$-$ 10 %

Table 6.4: Sensitivity analysis of the Bitzer coefficients

Results of Research Questions

7.1 Various Load

7.1.1 Variation in Load and the Influence in Boreholes in Model

Results from changing the ratio in the model is presented in table 7.1. The effect on the boreholes are presented in figure 7.1 and 7.2.

Load	**Change Qcl**	**Ratio**	**E_{max}/E_{min} [kJ]**	**T_{max} [°C]**	**$E_{balance}$ [kW]**	**SPF_{tot}[-]**
Load 1	Base Case	0.53	$1.11/1.10 \times 10^{12}$	7.1	1.21×10^{6}	1.0
Load 1	-50%	0.26	$1.11/1.10 \times 10^{12}$	7.4	1.59×10^{6}	1.0
Load 1	+50%	0.79	$1.10/1.08 \times 10^{12}$	6.2	-4.77×10^{6}	1.0
Load 2	Base Case	0.29	$1.38/1.36 \times 10^{11}$	10.6	1.57×10^{5}	5.0
Load 2	+50%	0.44	$1.39/1.36 \times 10^{11}$	11.4	1.39×10^{5}	5.4
Load 2	+150%	0.74	$1.39/1.36 \times 10^{11}$	12.4	1.33×10^{5}	6.3

Table 7.1: Results for changing energy ratio of cooling and heating demand tested in model by reducing cooling load

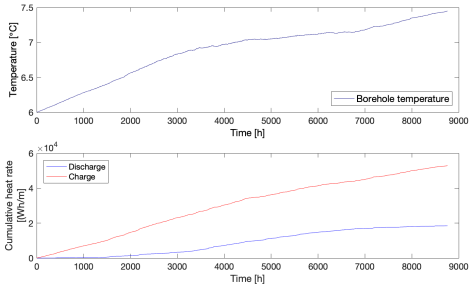

(a) Borehole storage with cooling over heating ratio of 0.26

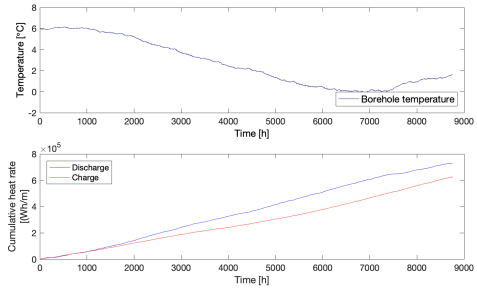

(b) Borehole storage with cooling over heating ratio of 0.79

Figure 7.1: Temperature and cumulative diagram for Load 1 when changing the ratio

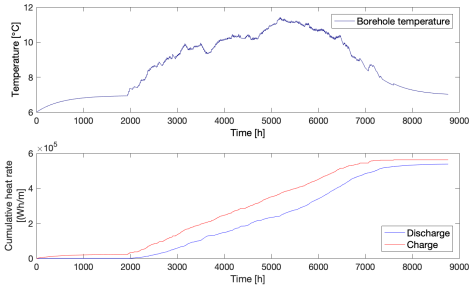

(a) Borehole storage with cooling over heating ratio of 0.44

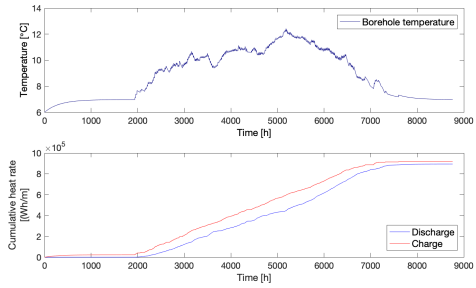

(b) Borehole storage with cooling over heating ratio of 0.74

Figure 7.2: Temperature and cumulative diagram for Load 2 when changing the ratio

For Load 1 the boreholes do not respond as desired at all. For Load 2 the results are more reasonable, the maximum temperature in the boreholes increase with increased cooling load and the total SFP in the system increases at the heat pump cover a larger cooling demand.

7.1.2 Variation in Load and the Influence in Boreholes in EED

The black line represent the fluid temperature and the green present the specific heat extraction.

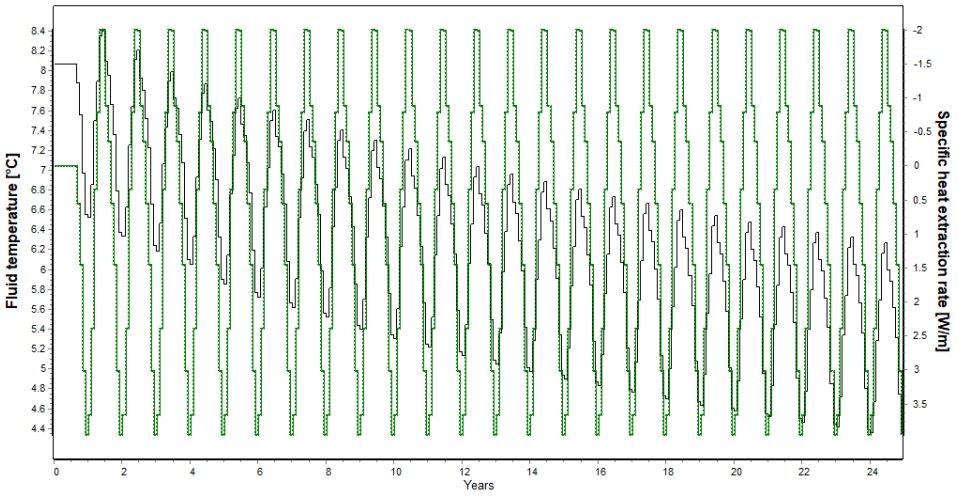

Figure 7.3: Load 1: Result from EED, ratio=0.53

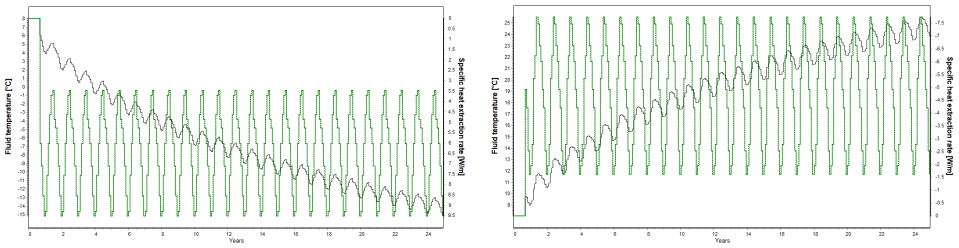

(a) Load 1: Result from EED, ratio=0.26 **(b)** Load 1: Result from EED, ratio=0.79

Figure 7.4: Fluid temperature and specific heat extraction for Load 1 using EED

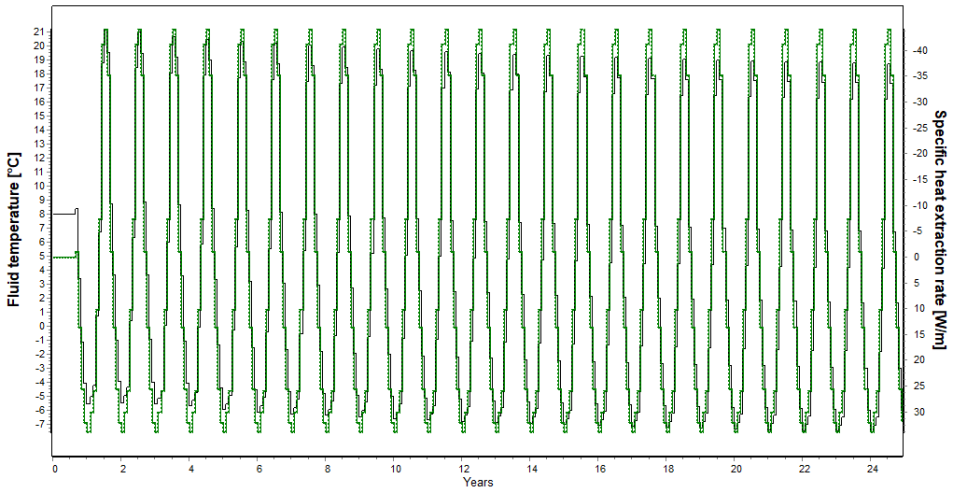

Figure 7.5: Load 2: Result from EED, ratio=0.44

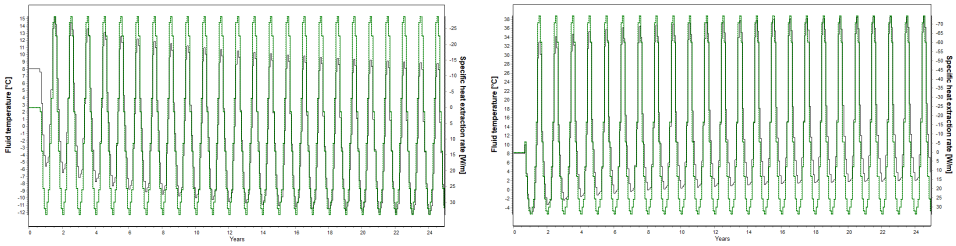

(a) Load 2: Result from EED, ratio=0.29 **(b)** Load 2: Result from EED, ratio=0.74

Figure 7.6: Fluid temperature and specific heat extraction for Load 2 using EED

Relatively small yearly temperature differences for Load 1. Large yearly temperature difference for Load 2. For both loads the cooling over heating ratio around 0.5 provide the most stable result over 25 years.

7.2 Sizing of Thermal Energy Storage

7.2.1 Sizing The Water Storage Tank

The result of using the minimum operating step method is presented by the temperature level in the water storage tank in figure 7.7, 7.8 and 7.9.

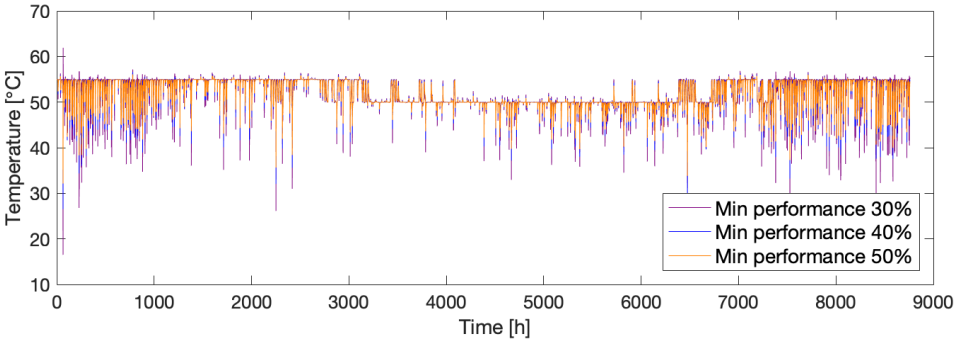

Figure 7.7: Temperature in tank at residence time 2h, 3h, 4h, 5h

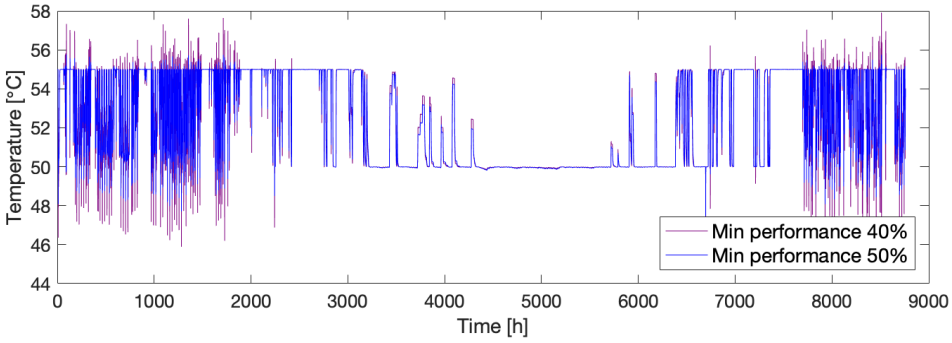

Figure 7.8: Temperature in tank at residence time 2h, 3h, 4h, 5h - zoomed in

Note that the temperature development in the tank for Load 2 is much better than in the base case where the temperature in the tank was decreasing over time. When the minimum operating step was 20 % a mistake occurs for both Load 1 and Load 2. The diagrams are presented in figure 7.9. It can be seen

that both loads achieve a low negative temperature and especially for Load 2 the maximum and minimum temperature is way out of range.

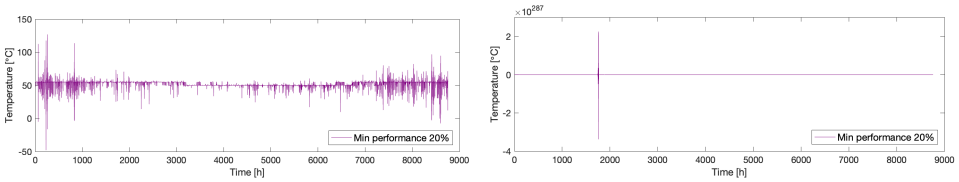

(a) Load 1 **(b)** Load 2

Figure 7.9

The results for sizing the water storage tank using the residence time method are presented below if figure For Load 1 the nominal flow of the heating system is equal to 5.83 kg/s and for Load 2 it is 0.97 kg/s.

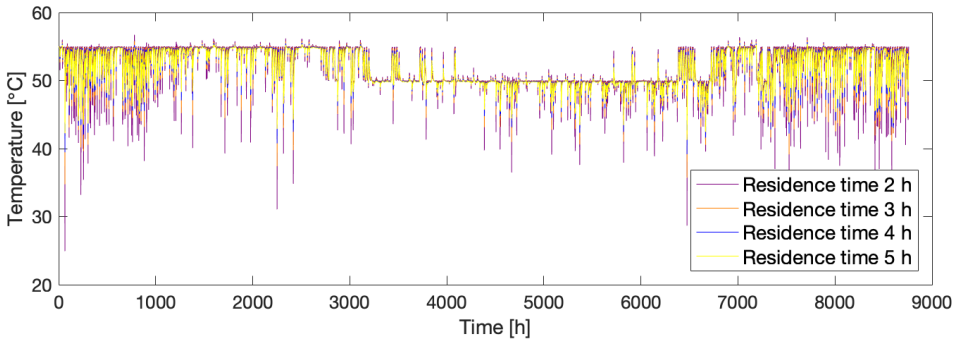

Figure 7.10: Load 1:Temperature in tank at residence time 2h, 3h, 4h, 5h

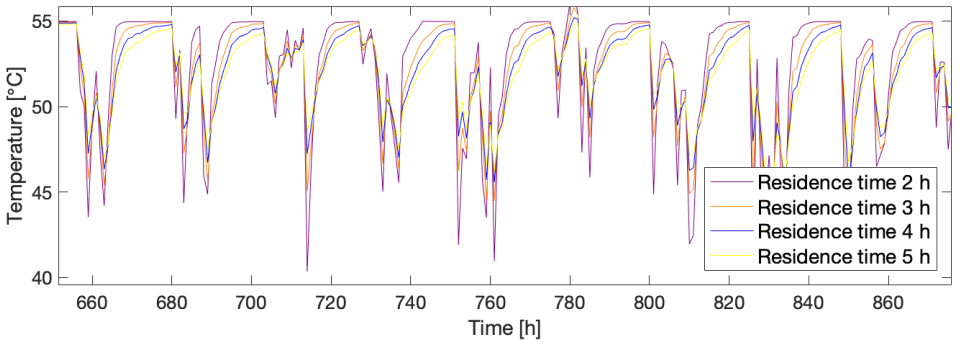

Figure 7.11: Load 1: zoomed in

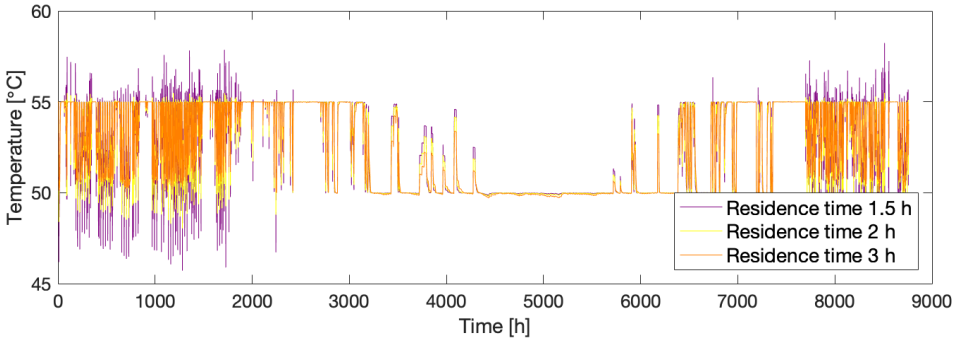

Figure 7.12: Load 2: Temperature in tank at residence time 1.5 h, 2h, 3h

The results show that the longer residence time the more accurate temperature in the tank. When the graph is zoomed is it can be observed that the smallest tank size give the most rapid changes, but this also result in larger deviation from the desired temperature in the tank. The sizing methods provide smaller volume of the tank than the assumed volume in the base case. For Load 2 especially this results better temperature development over the year. When the tank become to small, the calculations are not good.

7.2.2 Sizing the Borehole Configuration

The volume of the boreholes is increased and reduced. Table **??** shows the the influence on the temperature difference from changing the volume.

Load	Change of volume	Temperature difference	Temperature change in %
Load 1	Base Case	1.15	-
Load 1	+10%	1.08	-6.1%
Load 1	+50%	0.87	-24.3%
Load 1	−10%	1.23	+7.0%
Load 1	−50%	1.79	+55.7%
Load 2	Base Case	4.64	-
Load 2	+10%	4.50	-3.0%
Load 2	+50%	4.07	-12.3%
Load 2	−10%	4.80	+3.4%
Load 2	−50%	5.60	+20.7%

Table 7.2: Temperature difference in boreholes when changing volume

By reducing the volume of the borehole storage, the seasonal temperature difference over the year increases as expected.

7.3 Temperature levels

The strategy where the return temperature on the secondary side of the condenser increases with decreasing outdoor temperature is tested in the model to see how this temperature level influence the performance. The result is presented in figure 7.13 and 7.14. The figures show a reduced performance of the heat pump when the temperature is too high, not strange when the temperatures are out of range.

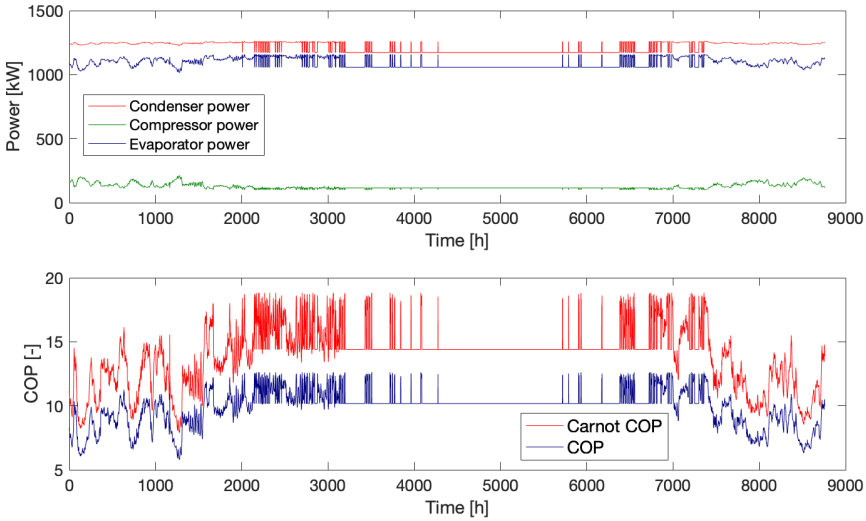

Figure 7.13: Load 1: Performance in system when temperature level increase by decreasing T_{out}

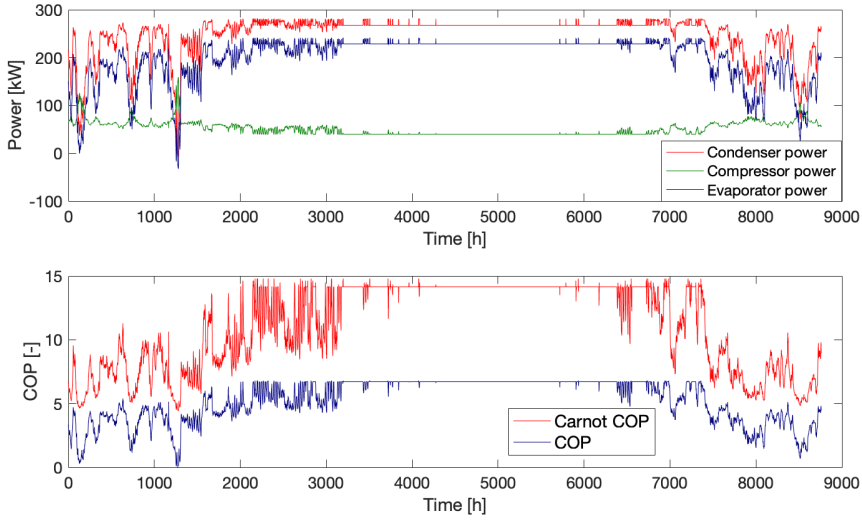

Figure 7.14: Load 2: Performance in system when temperature level increase by decreasing T_{out}

7.3.1 Influence on Boreholes and Performance due to Reduction in Temperature Level in Cooling System with 4 °C

Parameter	Name	Value	Unit
Average compressor power	P_{comp}	130.2	kW
Average condenser power	P_{cond}	1061.1	kW
Average compressor power	P_{evap}	932.5	kW
Seasonal Performance Factor	SPF	8.1	-
Carnot, Seasonal Performance Factor	SPF_{carnot}	11.2	-
Maximum/minimum temperature in boreholes	$T_{bh,max}$	6/4.2	°C
Average temperature in boreholes	$T_{bh,avg}$	5.0	°C

Table 7.3: Load 1

Parameter	Name	Value	Unit
Average compressor power	P_{comp}	38.8	kW
Average condenser power	P_{cond}	246.6	kW
Average compressor power	P_{evap}	208.3	kW
Seasonal Performance Factor	SPF	6.4	-
Carnot, Seasonal Performance Factor	SPF_{carnot}	12.9	-
Maximum/minimum temperature in boreholes	$T_{bh,max}$	7.6/3.4	°C
Average temperature in boreholes	$T_{bh,avg}$	5.3	°C

Table 7.4: Load 2

The temperature difference in the boreholes increases when reducing the temperature in the cooling system. The performance of the system was reduced as the temperature lift was increased.

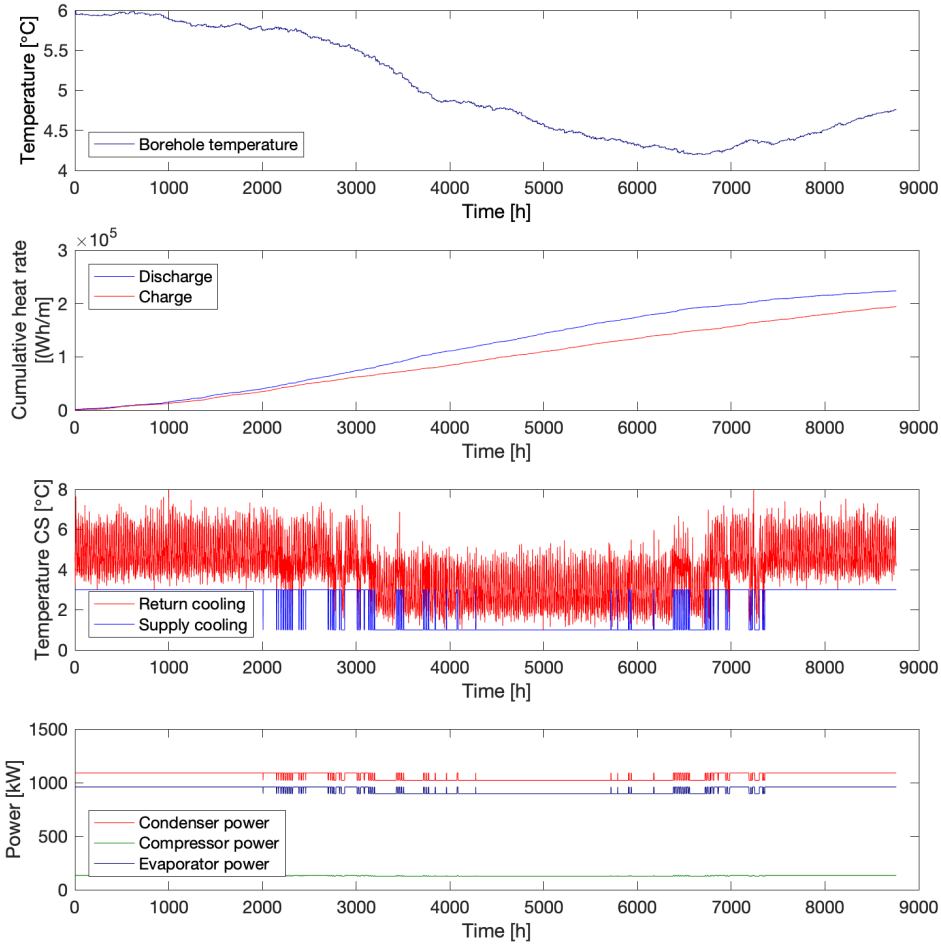

Figure 7.15: Temperature level in borehole storage reducing the temperature level in the evaporator circuit by 4 °C

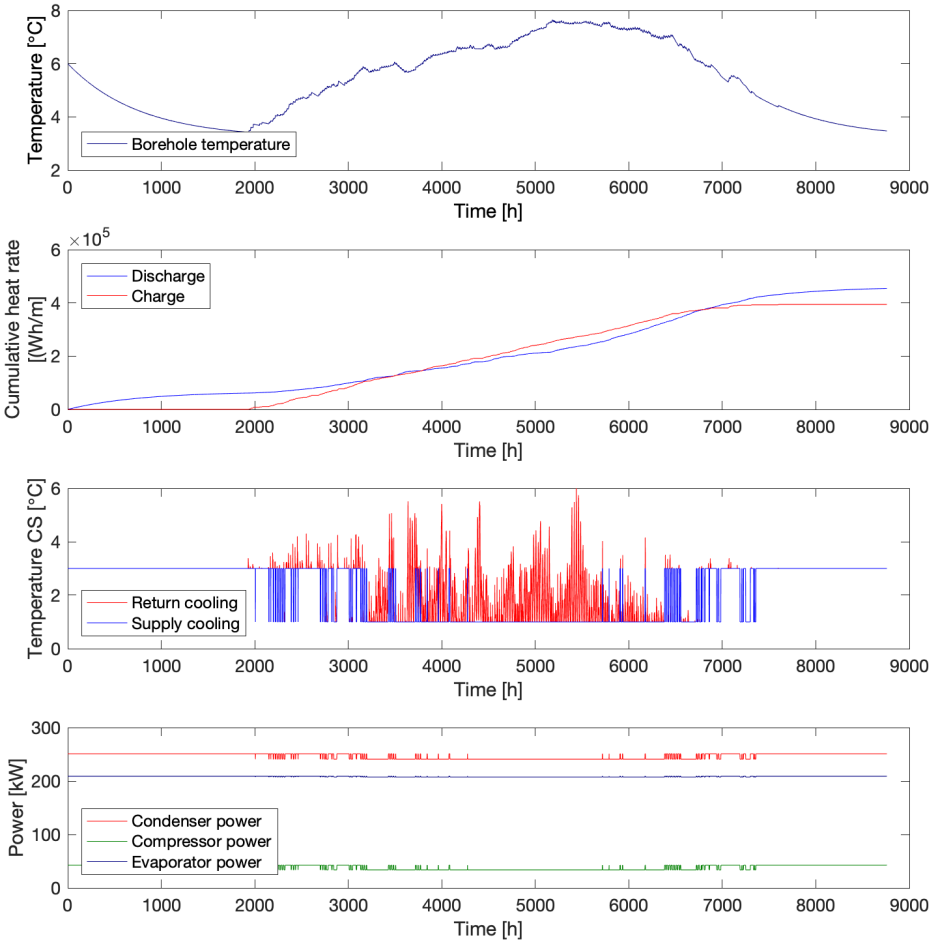

Figure 7.16: Borehole temperature when reducing the temperature level in the evaporator circuit by 4 °C

From the temperature development in the boreholes it can be seen that when the temperature in the cooling system is reduced the assumption for the initial temperature in the borehole storage is not good. The initial temperature in the boreholes are changed to $T_{boreholes}(1) = 3°C$. The results are presented in figure 7.17 and 7.18.

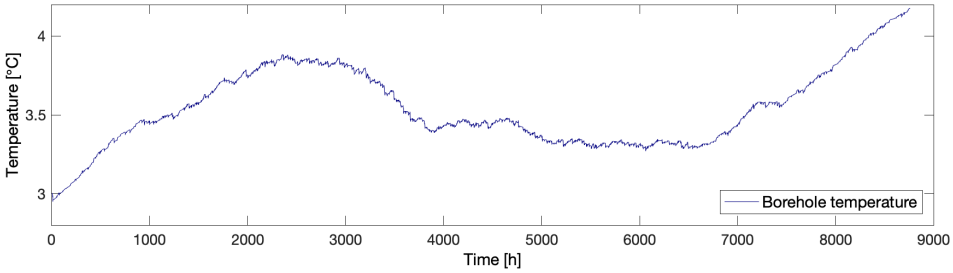

Figure 7.17: Load 1: Borehole temperature development when $T_{boreholes}(1) = 3°C$

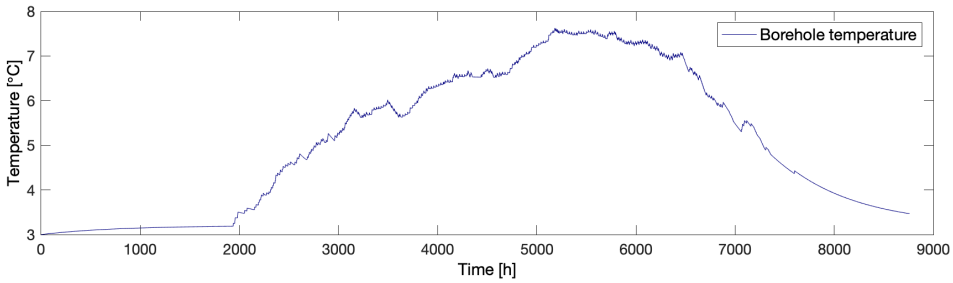

Figure 7.18: Load 2: Borehole temperature development when $T_{boreholes}(1) = 3°C$

By reducing the temperature in the cooling system the performance of the system is reduced, at the temperature lift for the compressor become larger. The temperature development in the boreholes for Load 1 is not improved, but for Load 2 the temperature difference is increased.

7.4 Choice of compressor

The performance of the heat pump in the model is a function of the preset evaporator and condenser temperature. Each compressor type is testes with the base case temperatures to test the performance for each compressor. The results are shown in figure 7.19. Note that the seasonal performance factor is

significantly larger than the COP given by the manufacturer. For model W6FA-K, 4NSL-30K and 6CTE-50K the temperature levels in the base case are out of their operating range and this can have an effect on the performance. Especially for W6FA-K, the SPF is unlikely high.

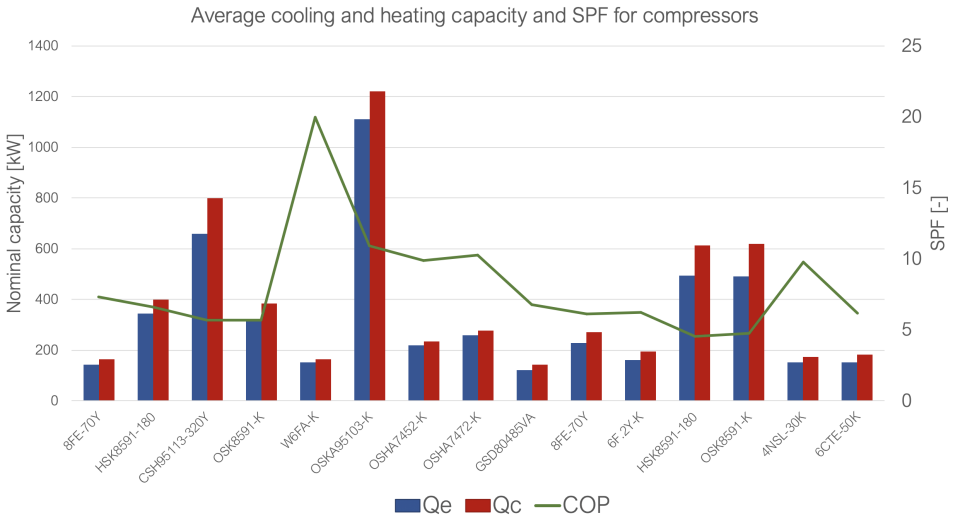

Figure 7.19: Compressor performance with temperature level from Base Case

Compressor CSH95113-320Y is tested with different temperature levels in its operating range to see how the temperatures and the temperature lift impact the performance.

Temperature lift	**$T_{r,cond}/T_{r,evap}$**	**Unit**	**SPF**	**Q_{cond}**	**Q_{evap}**	**P_{com}**
Base Case	55/5	°C	5.29	761.33	617.43	143.99
+10°C	60/0	°C	4.40 ↓	634.59 ↓	490.22 ↓	144.28 ↑
-10°C	50/10	°C	6.55 ↑	918.08 ↑	779.12 ↑	140.08 ↓

Table 7.5: Change in temperature lift to influence the performance

When the temperature lift is reduced by 10 %, the performance increases by 23.8 %.

7.5 Control of thermal energy storage

7.5.1 No Control in Water Storage Tank

The results of implementing no control of the borehole storage are presented in figure 7.20 and 7.21.

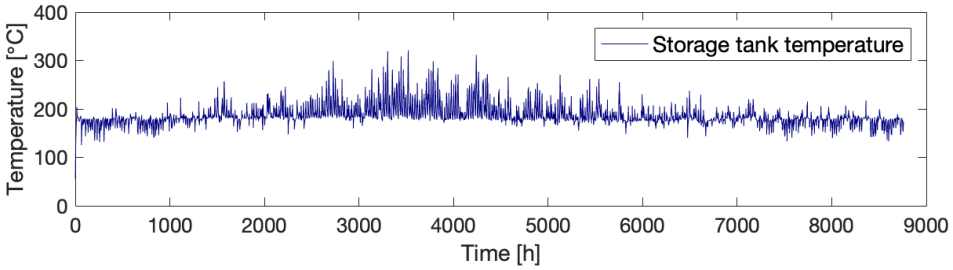

Figure 7.20: Load 1: No control in water storage tank

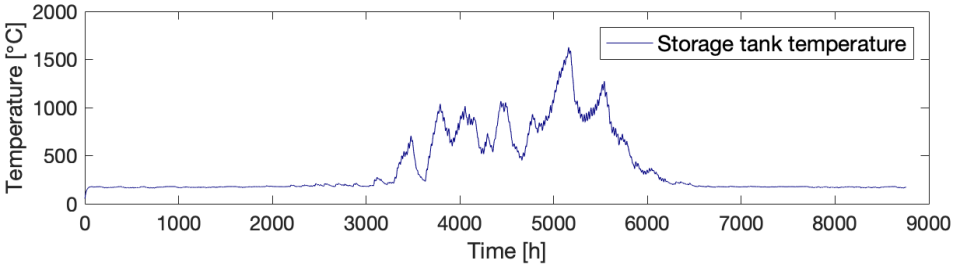

Figure 7.21: Load 2: No control in water storage tank

The results of implementing no control in the water storage tank are not good. The temperatures are too high and it seems like there is a mistake in the model.

7.5.2 Demand Controlled Borehole Storage

The demand control for the borehole storage was used in the base case of the models from 5 it can be seen that demand control work well for Load 2, while Load 1 is not responding as expected.

7.5.3 Seasonal controlled borehole storage

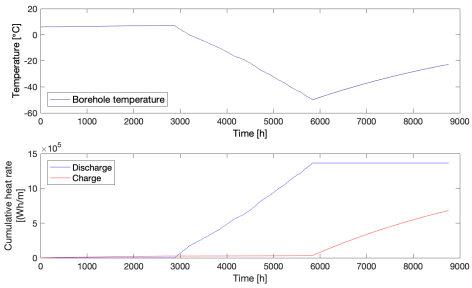

(a) Borehole storage with cooling over heating ratio of 0.26

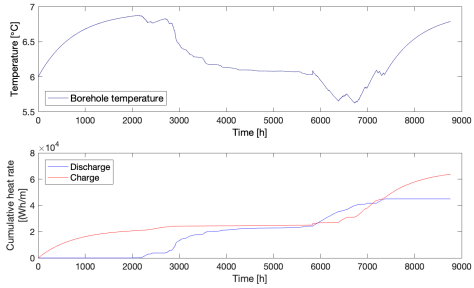

(b) Borehole storage with cooling over heating ratio of 0.79

Figure 7.22: Temperature and cumulative diagram for Load 2 when changing the ratio

The results of implementing seasonal control on the borehole storage do not respond as well as desired, there are no sign of energy balance in the system.

7.6 Result of Sensitivity Analysis

The thermal energy system consist of many assumptions and simplifications that causes uncertainties in the model. In this section a brief sensitivity analysis of the influence of the BITZER coefficients have been performed in order to evaluate the influence of an uncertain components in the model. The results of the sensitivity analysis of the BITZER coefficients are presented in table 7.6

Load 1: q, C, P, a	+/− 0 %	10.96	Change of SPF in %
q, C, P, a	+ 10 %	43.61	+398.0%
q, C, P, a	− 10 %	6.13	-44.1 %
Load 2: q, C, P, a	+/− 0 %	6.10	Change of SPF in %
q, C, P, a	+ 10 %	5.53	- 9.3%
q, C, P, a	− 10 %	6.60	+ 8.2%

Table 7.6: Sensitivity analysis of the BITZER coefficients

Increasing the coefiicients with 10 % for Load 1 results in an increase of SPF of 398 %.

Discussion

This chapter presents the discussion of the results that was achieved in the previous chapter. In the first part, the most important results are summarized. Second, the sub-models are evaluated and discussed. Then the limitations of the model are presented and the consequences of the limitations are discussed.

The goal of the masters thesis have been to establish a model of a ground source thermal energy system and use the model to perform analysis and evaluations of the system. Several research questions have been investigated in the model in order to improve the model and evaluate the thermal energy system. Simulations performed in Energy Earth Designer show that the ratio between the heating and cooling demand have significance for the energy balance in the boreholes. Various load in the model also demonstrate that the SPF_tot is higher with a higher cooling demand. The sizing of the thermal energy storages have great influence on the behaviour of the storage and the response of the changes. The boreholes that act as a seasonal thermal energy storage with a large volume responds slower than the storage tank that act as a short term energy storage which have an immediate response to changes. The temperature difference in the boreholes is small, and by reducing the volume the temperature difference increase. The temperature levels of the heating and cooling system have a great influence on the system performance and a low temperature lift for the compressor results in improved overall performance. The heating system is evaluated with different strategies for deciding the heating system temperature. When the return temperature from the condenser is increased with reduced outdoor temperature the performance of the heat pump is reduced. The temperature level of the cooling system is analyzed in regard to the temperature level in the boreholes. The temperature development in the boreholes with Load 2 is more realistic when the return temperature from the evaporator is reduced by 4 °C. The temperature development in the boreholes for Load 1 are not responding as desired. Demand control and seasonal control of the borehole storage have been interpreted in the model. The results are significantly bet-

ter with demand control, even for Load 2 with large seasonal differences. The compressors obtained from BITZER provide very high COP and SPF for the heat pump. The sensitivity analysis demonstrate that the changing the coefficients for compressor index 6 have large impact on the performance and the coefficients are very sensitive, but for the compressor index 10 the changes are more moderate and expected.

The model of the borehole storage deliver occasionally good results, especially together with Load 2 the borehole storage responds well to adjustments, and the results regularly meet the expectations. When the volume of the storage is reduced the temperature difference increase as the volume of mass to heat up is reduced. The borehole storage with Load 2 works well with the demand control strategy that is implemented. The seasonal control of the borehole storage do not present as good results as expected. It was expected that the seasonal control of the borehole storage would work well with Load 2 as the load have large seasonal differences. A pervasive result in the model is that the borehole storage does not respond as intended when Load 1 is implemented. There are not obtained a convinced reason for this in the thesis, but the combination of a simplified model and a too general control strategy of the borehole storage are most certainly impacting the result. From the EED simulation it can be observed that the temperature development in such a borehole storage over several years would have a larger seasonal temperature differences with a higher temperature during summer season and a lower temperature during winter season. For Load 1 EED presents a very stable borehole storage. For Load 1 a better control strategy could possibly improved the results. The simplifications in the borehole storage model most definitely impact the results. The influence of each borehole to the ground is not possible to evaluate. As the flows for each borehole is connected to one large inflow and outflow the temperature distribution become more concentrated for a small area, and the temperature distribution is not as even as it is in an actual borehole storage. Figure 8.1 presents three various alternatives for the effect from the boreholes to the ground. To improve the borehole storage a more detailed model must be implemented. Claesson et al. (2011) presents a method to calculate each borehole as separate units in a mesh grid, this method is transferable to MATLAB. Another solution would be to model the borehole sub-model in another simulation program that include ground heat exchanger models as for example TRNSYS and then implement a

co-working technique to build the overall thermal energy system.

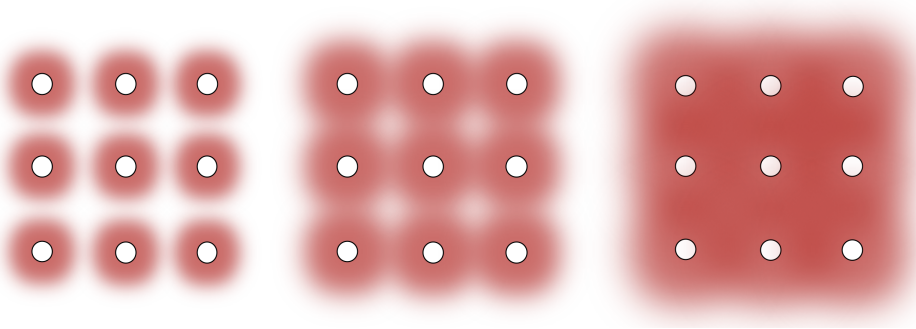

Figure 8.1: Three alternatives of the effect of the heat from the boreholes to the surrounding ground

The research aimed to identify the influence of variations in the heating and cooling demand. The results from reducing the cooling load and thereby increasing the cooling over heating ratio. For Load 1 the results did not meet the expectations as the borehole model did not respond well to Load 1. The total Seasonal Performance Coefficient SPF_{tot} is increased when the cooling demand increases as the system cover a larger cooling demand without large.

The sub-model of the water storage tank works very well when the sizing and control is good. For both loads the water storage tank act as a short term energy that supply the heating system with even temperatures. Since the water storage tank is not overly complex the simple control volume and discretization over hourly time steps seems to be a good interpretation. When the tank is small the response time is rapid, but the best temperature level is obtained when the tank is a bit larger, for example with a response time of two hours. For future modeling of water storage tanks it should be considered modeling the more common tank with four pipes instead of three. That would make it easier to interpret several layers.

The sub-model of the heat pump provide good calculations for the performance of the heat pump. The performance of the heat pump is very high regardless of compressor choice and temperature choices. The high performance calcu-

lations is a result of high condenser power and low compressor power in the model compared to the stated capacities from the manufacturer. The performance data of the heat pump is obtained from the regression model of the BITZER coefficients. Underwood (2016) states that a regression model performed from manufacturer data often will provide good results due to the environment of the calculations. The capacity calculations are often simulated in a idealized environment, as for example the BITZER Software, and the influence of layout and installation is not considered. Kim et al. (2013) also addresses the gap between idealized performance data and the actual performance. A regression model based on actual experimental data would probably provide more realistic results.

Madani et al. (2011) suggest a map for the complexity of a model figure 8.3, and suggests the required level of complexity compared to the subject that is to be investigated in the model. The model of this master thesis investigate the overall system and the performance of the system from a yearly perspective. It does not include details from daily operation and neither the model of the heat pump unit nor the heat source are models of high complexity. The model is for this reason situated in Zone A, which describe the purpose of the model very well; comparative analysis of different control strategies in the system level.

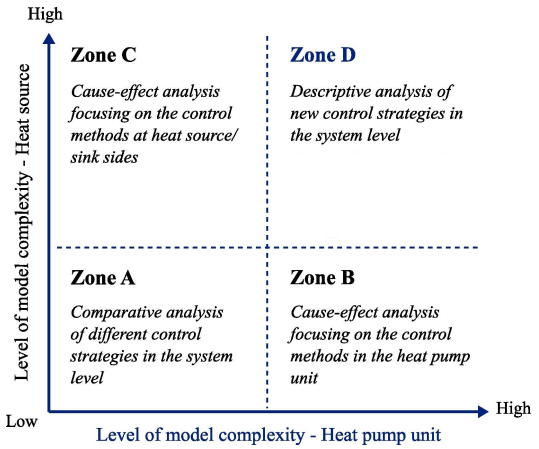

Figure 8.2: Model complexity (Madani et al. 2011)

The regression model of the BITZER coefficients provide some limitations in the heat pump model regarding the input parameters that can be used to calculate the performance of the heat pump. Since the capacity is calculated from the BITZER polynomials that are functions of specific parameters, the influence of other parameters can not be tested in the model. This limitation for regression models was presented by Underwood (2016) and for the model in this thesis, the exact problem presented itself when the influence of the return temperature in the heating system was supposed to be tested. Since the polynomials are not functions of the return temperature, the influence of the return temperature on the performance of the system can not be evaluated. This is a limitation for several parameters that in an actual system would influence the performance of the system.

The model consist of several uncertainties and assumptions. Rohde (2019) presents in his PhD thesis a diagram that shows the potential error in the predictions versus the model complexity.

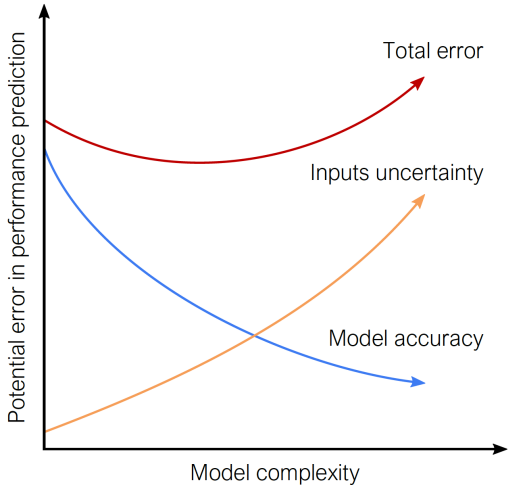

Figure 8.3: (Rohde 2019)

A thermal energy system is complex and there are many parameters that must work together. In the model of this master's thesis a lot of assumptions and

predictions are adapted in order to make a solution with limited input. The results from the thesis are various reflect the limitations of the model, some results are good while others are useless. The approach in this model have been to create several simplified sub-models, another approach that might would provide just as good results would be to start with modeling one component, and model it to a level certainty so that it would not be a source of uncertainty.

Conclusion

In this chapter a conclusion will be presented as well as recommodations for further work.

The main results show from this work have been that demand control of the borehole storage provide the best temperature development in the borehole storage, and a low temperature lift for the compressor provide good performance in the system. If the temperature lift become too large the performance reduced. This masters thesis show that overall analysis and evaluation of a thermal energy system integrating short- and long therm energy storage can be performed in a MATLAB model consisting of several sub-models. The work suggests a method and model for analyses and evaluation of a thermal energy system. The model provide quite good results for Load 2 and the temperature development in both the boreholes and the water storage tank behave as expected when changes are performed.

9.1 Recommendations for Further Work

The work of this thesis have been to develop a model in MATLAB of a thermal energy system with a heat pump and a borehole storage as heat source and use the model to perform various test various research questions, both for improving the model and to check the thermal energy system itself. To obtain a perfect model would require a lot more work and suggestions for further work is given below.

- The sub-models of this work deliver various results, improvements of the sub-models especially for the borehole storage would provide a better model. Improvements could be done by for example modeling each borehole in a mesh grid that take the surrounding boreholes into account. Improving the water storage tank could include modeling stratification

layers and make independent operation of the storage tank and the heating system possible.
- The connection of each sub-model could to a larger degree include pumps and valves for more detailed operation.
- The manufacturer performance data should be compared to actual measurements to obtain performance results for a more realistic system.
- Transfer the thermal energy system to more detailed simulation and modeling software or implementing Simulink/Carnot package in MATLAB.

Bibliography

Aaberg, Marie Garen (2018). *Analyse av det termiske energisystemet ved KIWI Dalgård*.

— (2019). *Analyse av det termiske energiforsyning ved SWECO-bygget*.

Alfstad, Linn Charlotte Melvik (2018). *Analyse av termisk energiforsyning ved Otto Nielsens vei 12E*.

Alimohammadisagvand, Behrang, Juha Jokisalo and Kai Sirén (2018). 'Comparison of four rule-based demand response control algorithms in an electrically and heat pump-heated residential building'. In: *Applied Energy* 209, pp. 167–179.

BITZER (2020). *About us*. URL: `https://www.bitzer.de/gb/en/about-us/` (visited on 20/03/2020).

BITZER Group (20th Mar. 2020). *BITZER Software*. Version 6.15.0. URL: `https://www.bitzer.de/websoftware/Default.aspx`.

Cadau, Nora, Andrea De Lorenzi, Agostino Gambarotta, Mirko Morini and Michele Rossi (2019). 'Development and Analysis of a Multi-Node Dynamic Model for the Simulation of Stratified Thermal Energy Storage'. In: *Energies* 12.22, p. 4275.

Carlucci, Salvatore (2019). *BOUNDARY CONDITIONS FOR BUILDING SIMULATION MODELS - Weather data, electric power for lighting and electric appliances, occupants - slides in course TBA4166*.

Claesson, Johan and Saqib Javed (2011). 'An analytical method to calculate borehole fluid temperatures for time-scales from minutes to decades'. In: *ASHRAE Transactions*. Vol. 117. 2, pp. 279–288.

Faanes, Audun and Sigurd Skogestad (2003). 'Buffer tank design for acceptable control performance'. In: *Industrial & engineering chemistry research* 42.10, pp. 2198–2208.

Haugen, Finn (2003). *Dynamiske systemer - modellering, analyse og simulering*. 3rd ed. Tapir Akademiske Forlag. ISBN: 82-519-1900-2.

IEA (2020). *Buildings - A source of enormous untapped efficiency potential*. https://www.iea.org/topics/buildings. Online; accessed 19 March 2020.

Kim, Jiyoung, Jea Chul Jang, Eun Chul Kang, Ki Chang Chang, Euy Joon Lee and Yongchan Kim (2013). 'Verification study of a GSHP system Manufacturer data based modeling'. In: *Renewable energy* 54, pp. 55–62.

Madani, Hatef, Joachim Claesson and Per Lundqvist (2011). 'Capacity control in ground source heat pump systems: Part I: modeling and simulation'. In: *International Journal of Refrigeration* 34.6, pp. 1338–1347.

Meisler, Anja (2020). *Analyse av termisk energiforsyning ved Moholt 50 50*.

Mibec (2020). *Bespoke Buffer Tanks*. URL: https://mibec.co.uk/products/thermal-storage/bespoke-buffer-tanks/ (visited on 16/03/2020).

NGU (2020a). *Brønnparker*. URL: https://www.ngu.no/grunnvanninorge/bore-en-bronn/energibronn/bronnparker (visited on 20/06/2020).

— (2020b). *Energibrønn*. URL: https://www.ngu.no/grunnvanninorge/bore-en-bronn/energibronn (visited on 20/06/2020).

Persson, Tomas, Ole Stavset, Randi Kalskin Ramstad, Maria Justo Alonso and Klaus Lorenz (2016). *Software for modelling and simulation of ground source heating and cooling systems*. Dalarna University, Department of Energy, Forrest et al.

Ramstad, Randi Kalskin (2017). *Energibrønner som varmekilde for varmepumper - Har kuldebransjen noe å lære her?*

Reuss, M (2015). 'The use of borehole thermal energy storage (BTES) systems'. In: *Advances in thermal energy storage systems*. Elsevier, pp. 117–147.

Rohde, Daniel (2019). *Dynamic Simulation of future integrated energy systems*.

Stene, Jørn (2019a). *Dimensjonering av varmepumper for oppvarming/kjøling - slides in course TEP 4260*.

— (2019b). *Komponenter for varmepumpeaggregater - slides in course TEP 4260*.

— (20th Feb. 2020). *Personal communication*.

Underwood, CP (2016). 'Heat pump modelling'. In: *Advances in Ground-Source Heat Pump Systems*. Elsevier, pp. 387–421.

Additional Material

A.1 Model Layout with MATLAB parameters

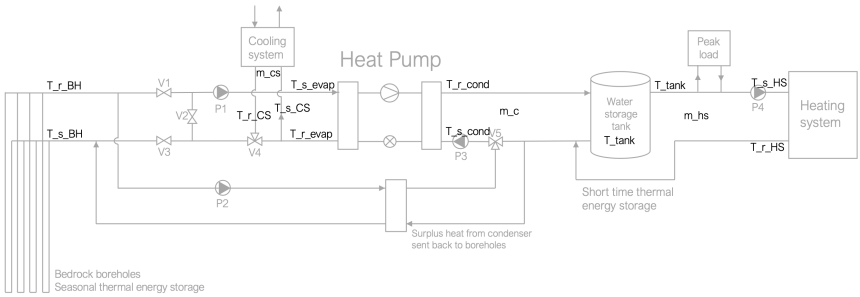

Figure A.1: Simplified system layout with MATLAB parameters.

A.2 Vulkan energy plant

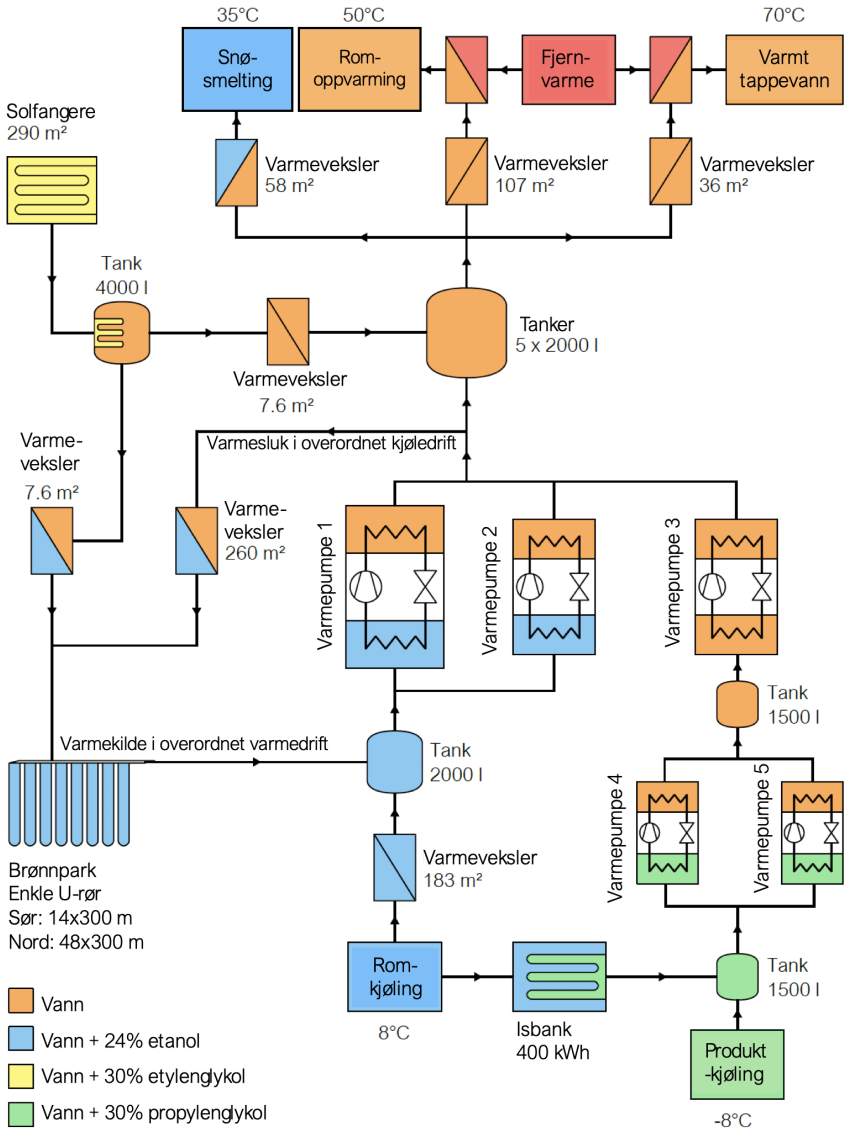

Figure A.2: Simplified system scheme of the thermal energy system at Vulkan energy plant (Rohde 2019)

A.3 SWECO building

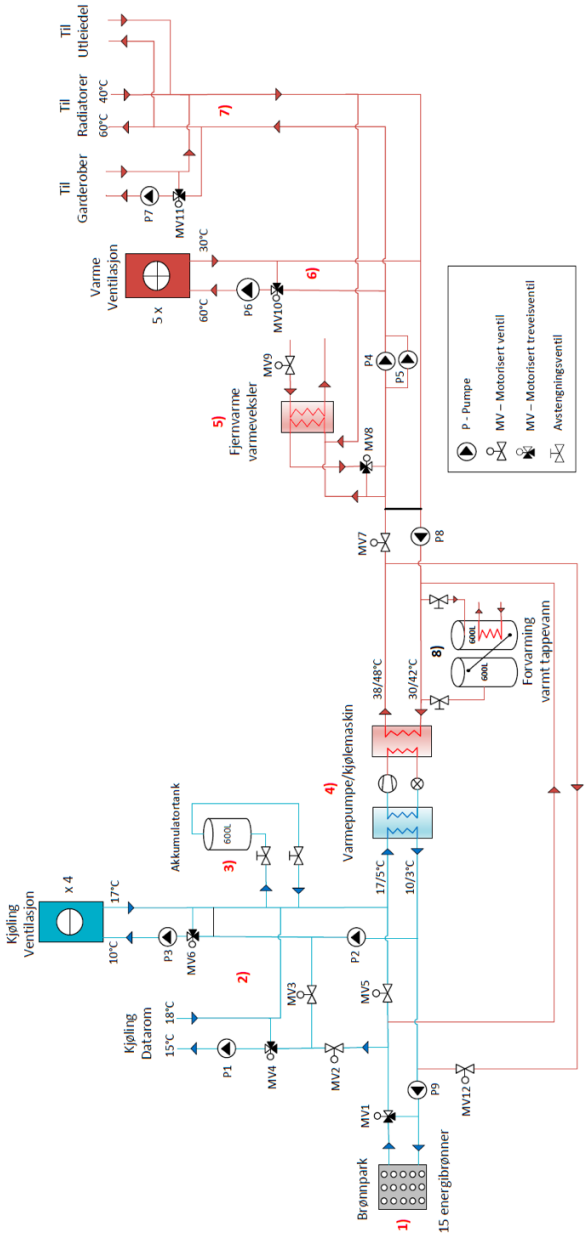

Figure A.3: Simplified system scheme of the thermal energy system at the SWECO building (Aaberg 2019)

A.4 Moholt 50 | 50

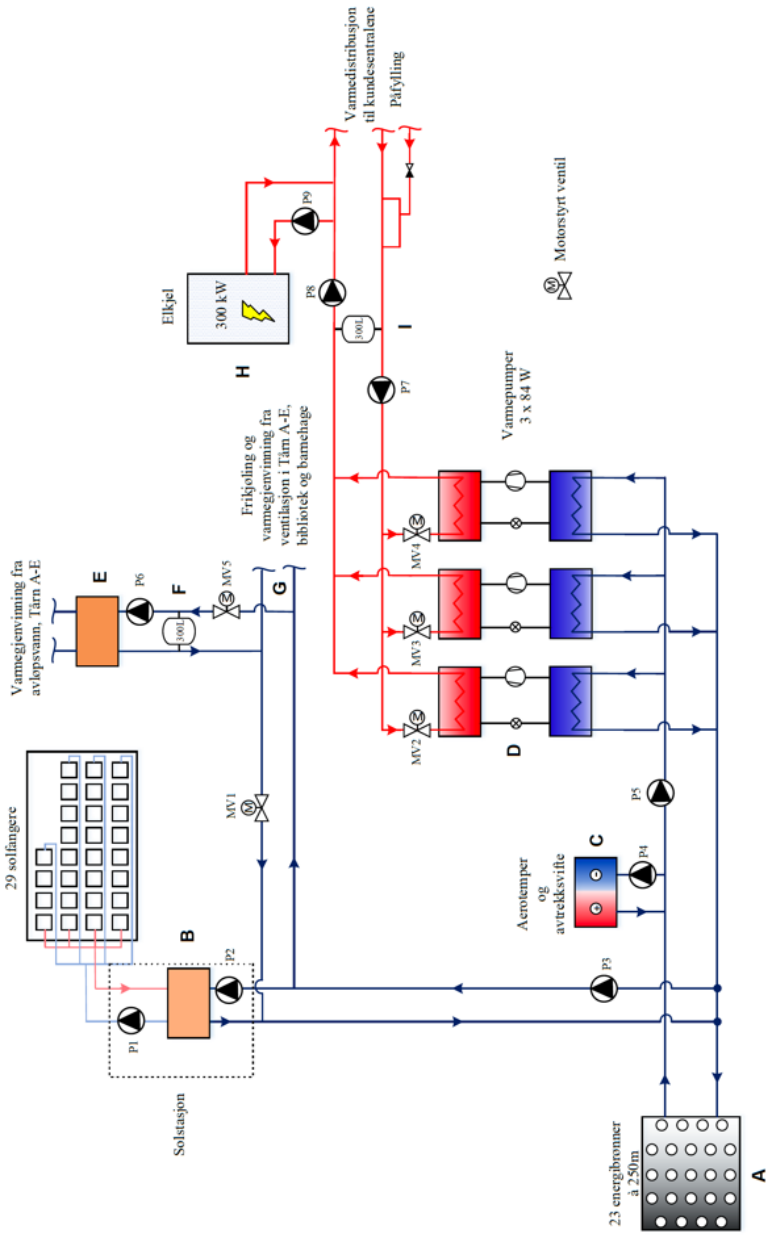

Figure A.4: Simplified system scheme of the thermal energy system at Moholt 50 |50 (Meisler 2020)

A.5 KIWI Dalgård

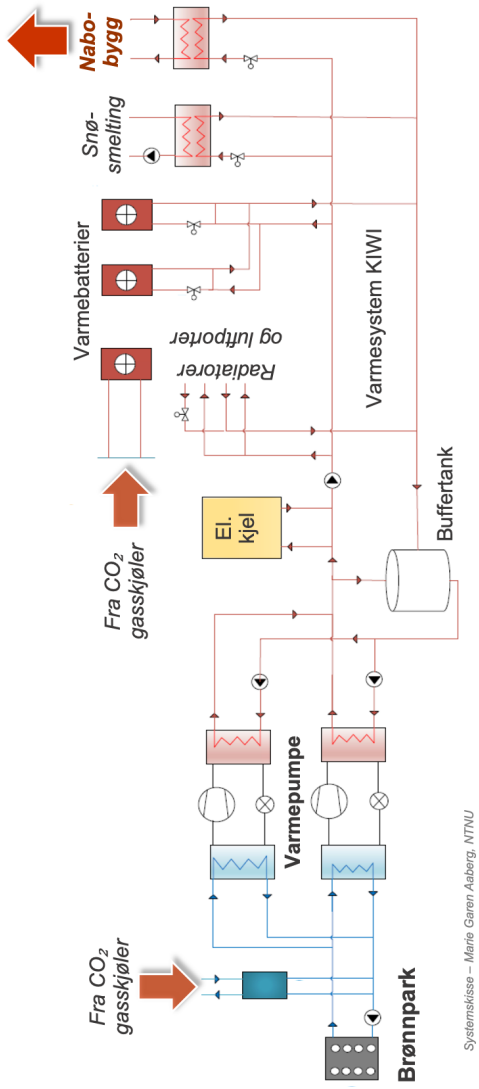

Figure A.5: Simplified system scheme of the thermal energy system at KIWI Dalgård (Aaberg 2018)

A.6 Otto Nielsens Vei 12 E

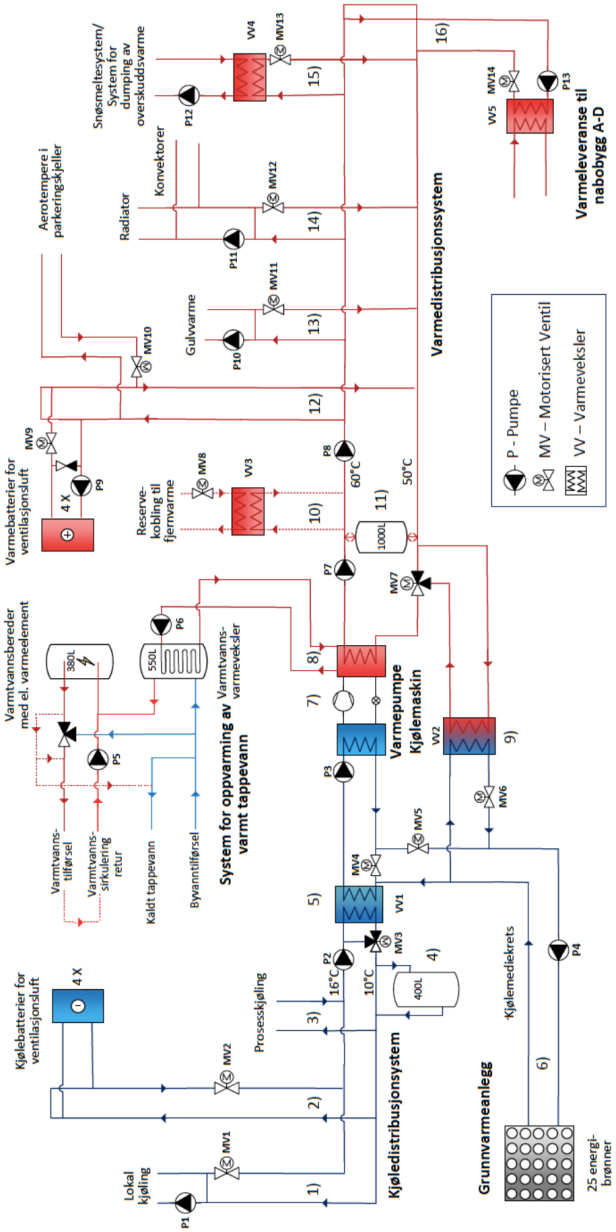

Figure A.6: Simplified system scheme of the thermal energy system at Otto Nielsens vei 12 E (Alfstad 2018)

A.7 EED output file

EED 4.19 - www.buildingphysics.com - license for wenche.w.finseth@ntnu.no
  Input file:UNTITLED.DAT
  This output file: UNTITLED.OUT Date: 6/24/2020 Time: 3:01:32 PM

MEMORY NOTES FOR PROJECT
[]

QUICK FACTS

Cost	-
Number of boreholes	160
Borehole depth	290 m
Total borehole length	4.64E4 m

D E S I G N D A T A

GROUND

Ground thermal conductivity	3.5 W/(m·K)
Ground heat capacity	2.38 MJ/(m³·K)
Ground surface temperature	6 °C
Geothermal heat flux	0.05 W/m²

BOREHOLE

Configuration:	598 ("160 : 10 x 16 rectangle")
Borehole depth	290 m
Borehole spacing	6 m
Borehole installation	Single-U
Borehole diameter	110 mm
U-pipe diameter	32 mm
U-pipe thickness	3 mm
U-pipe thermal conductivity	0.42 W/(m·K)
U-pipe shank spacing	70 mm
Filling thermal conductivity	0.6 W/(m·K)
Contact resistance pipe/filling	0 (m·K)/W

THERMAL RESISTANCES

Borehole thermal resistances are calculated.

Number of multipoles	10

Internal heat transfer between upward and downward channel(s) is considered.

HEAT CARRIER FLUID

Thermal conductivity	0.43 W/(m·K)
Specific heat capacity	4298 J/(Kg·K)
Density	971 Kg/m³
Viscosity	0.0045 Kg/(m·s)
Freezing point	-14.6 °C

Flow rate per borehole 0.55 l/s

BASE LOAD

Seasonal performance factor (DHW) 1
Seasonal performance factor (heating) 4
Seasonal performance factor (cooling) 3

Monthly energy values [MWh]

Month	Heat load	Cool load	Ground load
JAN	673	286	124
FEB	573	262	80.7
MAR	529	289	11.5
APR	455	277	−27
MAY	426	291	−68.2
JUN	403	278	−67.7
JUL	478	292	−30.1
AUG	493	287	−12.5
SEP	519	278	18.6
OCT	576	287	49.1
NOV	635	281	102
DEC	681	283	134
Total	6443	3389	314

PEAK LOAD

Monthly peak powers [kW]

Month	Peak heat	Duration	Peak cool	Duration [h]
JAN	200	100	0	0
FEB	200	100	0	0
MAR	200	100	0	0
APR	200	100	0	0
MAY	200	100	0	0
JUN	200	100	0	0
JUL	200	100	0	0
AUG	200	100	0	0
SEP	200	100	0	0
OCT	200	100	0	0
NOV	200	100	0	0
DEC	200	100	0	0

Number of simulation years 25
First month of operation SEP

C A L C U L A T E D V A L U E S
==========
∗ Monthly calculation ∗

Total borehole length 4.64E4 m

THERMAL RESISTANCES

Borehole therm. res. internal	0.63 (m·K)/W
Reynolds number	5822
Thermal resistance fluid/pipe	0.008782 (m·K)/W
Thermal resistance pipe material	0.07868 (m·K)/W
Contact resistance pipe/filling	0 (m·K)/W
Borehole therm. res. fluid/ground	0.1498 (m·K)/W
Effective borehole thermal res.	0.1583 (m·K)/W

SPECIFIC HEAT EXTRACTION RATE [W/m]

Month	Base load	Peak heat	Peak cool
JAN	3.66	3.23	0
FEB	2.38	3.23	0
MAR	0.34	3.23	0
APR	−0.8	3.23	0
MAY	−2.01	3.23	0
JUN	−2	3.23	0
JUL	−0.89	3.23	0
AUG	−0.37	3.23	0
SEP	0.55	3.23	0
OCT	1.45	3.23	0
NOV	3	3.23	0
DEC	3.95	3.23	0

BASE LOAD: MEAN FLUID TEMPERATURES (at end of month) [°C]

Year	1	2	5	10	25
JAN	8.07	6.53	6.05	5.4	4.36
FEB	8.07	6.86	6.34	5.71	4.67
MAR	8.07	7.5	6.93	6.33	5.29
APR	8.07	7.9	7.31	6.72	5.69
MAY	8.07	8.36	7.77	7.2	6.17
JUN	8.07	8.42	7.87	7.31	6.27
JUL	8.07	8.1	7.6	7.03	6
AUG	8.07	7.95	7.49	6.91	5.89
SEP	7.88	7.66	7.21	6.64	5.61
OCT	7.56	7.36	6.9	6.33	5.31
NOV	6.97	6.79	6.33	5.76	4.75
DEC	6.55	6.38	5.9	5.34	4.34

BASE LOAD: YEAR 25
Minimum mean fluid temperature 4.34 °C at end of DEC
Maximum mean fluid temperature 6.27 °C at end of JUN

PEAK HEAT LOAD: MEAN FLUID TEMPERATURES (at end of month) [°C]

Year	1	2	5	10	25
JAN	8.07	6.65	6.18	5.53	4.49
FEB	8.07	6.61	6.09	5.46	4.42

MAR	8.07	6.65	6.08	5.47	4.44
APR	8.07	6.71	6.12	5.54	4.5
MAY	8.07	6.81	6.23	5.66	4.62
JUN	8.07	6.88	6.33	5.77	4.73
JUL	8.07	6.89	6.39	5.82	4.79
AUG	8.07	6.89	6.43	5.85	4.83
SEP	7.09	6.87	6.42	5.85	4.83
OCT	7.03	6.83	6.38	5.8	4.79
NOV	6.91	6.73	6.26	5.69	4.68
DEC	6.76	6.59	6.11	5.55	4.55

PEAK HEAT LOAD: YEAR 25
Minimum mean fluid temperature 4.42 °C at end of FEB
Maximum mean fluid temperature 4.83 °C at end of AUG

PEAK COOL LOAD: MEAN FLUID TEMPERATURES (at end of month) [°C]

Year	1	2	5	10	25
JAN	8.07	6.53	6.05	5.4	4.36
FEB	8.07	6.86	6.34	5.71	4.67
MAR	8.07	7.5	6.93	6.33	5.29
APR	8.07	7.9	7.31	6.72	5.69
MAY	8.07	8.36	7.77	7.2	6.17
JUN	8.07	8.42	7.87	7.31	6.27
JUL	8.07	8.1	7.6	7.03	6
AUG	8.07	7.95	7.49	6.91	5.89
SEP	7.88	7.66	7.21	6.64	5.61
OCT	7.56	7.36	6.9	6.33	5.31
NOV	6.97	6.79	6.33	5.76	4.75
DEC	6.55	6.38	5.9	5.34	4.34

PEAK COOL LOAD: YEAR 25
Minimum mean fluid temperature 4.34 °C at end of DEC
Maximum mean fluid temperature 6.27 °C at end of JUN

Vilde Eikeskog

Analyses and Evaluation of the Heat Pump Based Energy Supply System Integrating Short- and Long Term Storages

NTNU
Norwegian University of
Science and Technology